



GiP

Learning geometry

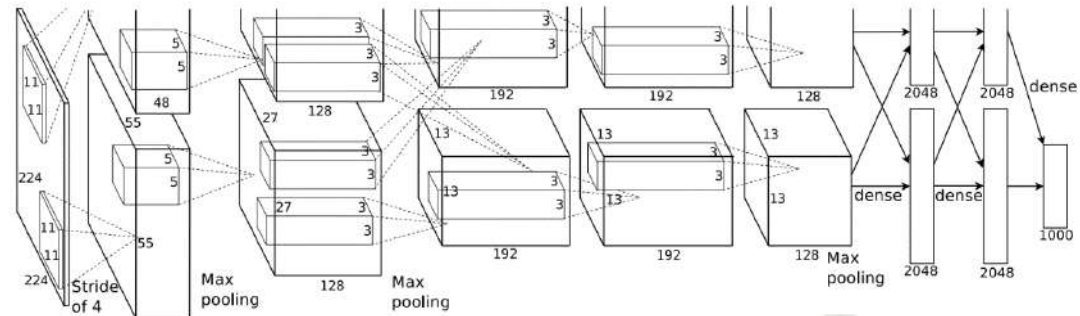
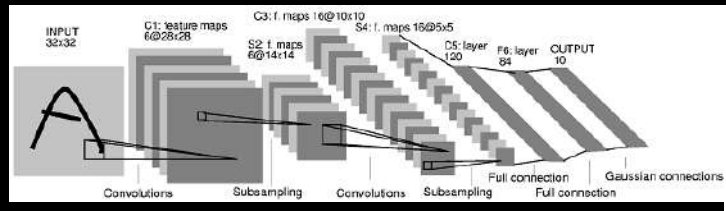
Ron Kimmel

Geometric Image Processing Lab.
Technion - Israel Institute of Technology

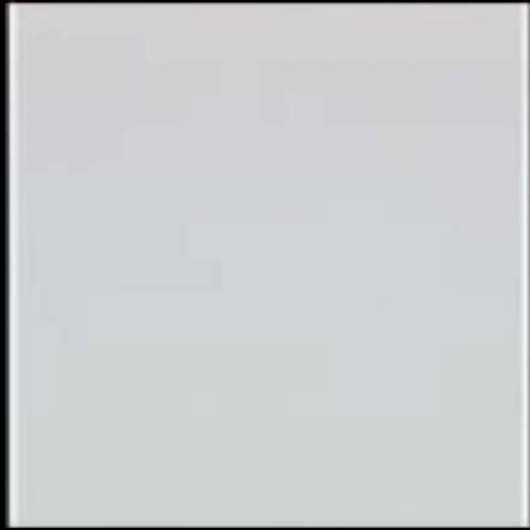
intel REALSENSE
TECHNOLOGY



Mathematical Methods for Objects
Reconstruction: from 3D Vision to 3D Printing
INdAM Workshop. Rome Feb. 10, 2021



3DMM



Vetter & Blanz, A morphable model for the synthesis of 3D faces, Siggraph 1999
Kemelmacher & Basri, 3D face reconstruction from a single image ... PAMI 2011

Learning using Axiomatic Knowledge

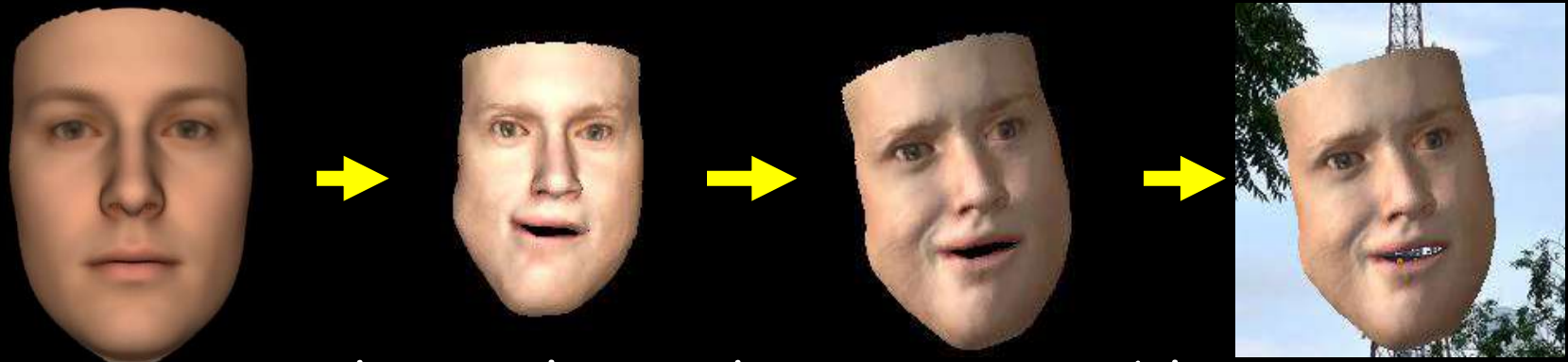


Learning using Axiomatic Knowledge

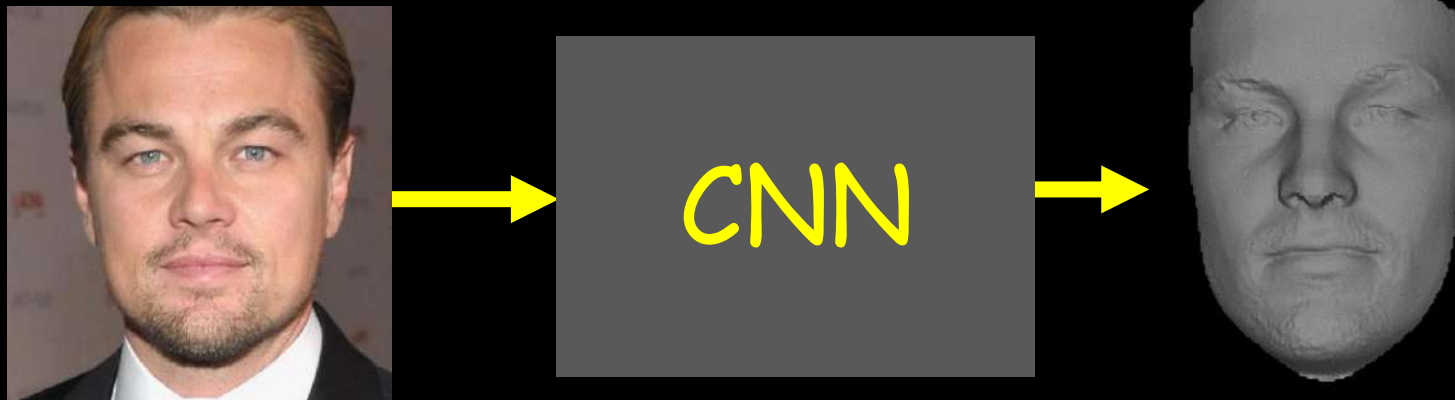


Learning using Axiomatic Knowledge

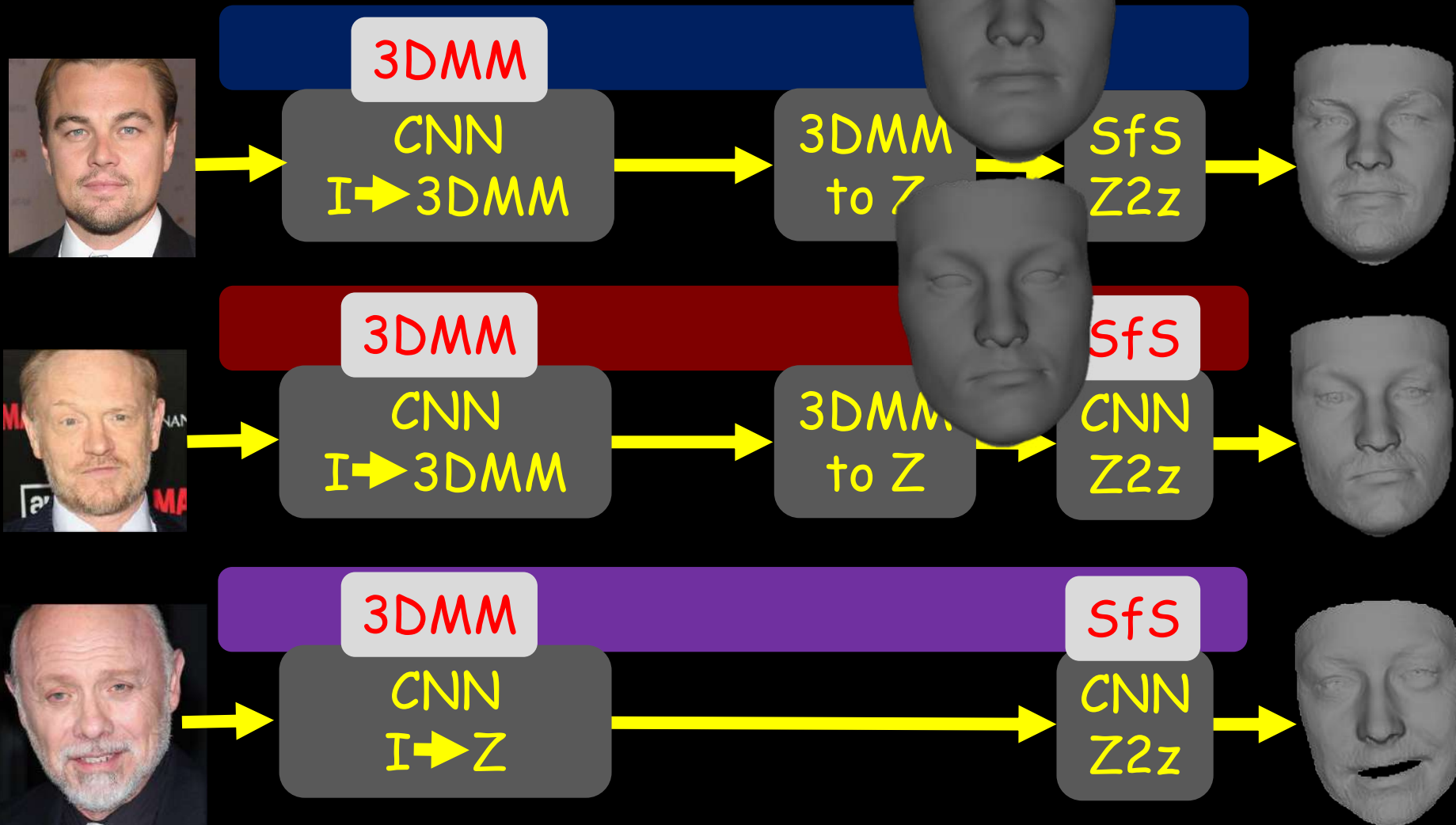
We know how to model faces



Can we use that to learn the inverse problem?



Face reconstruction evolution



input 2D image



output 3D face



output 3D face
with texture





Shamai, Slossberg, K. 2018/2019 Synthesizing photometries and geometries with GANs &



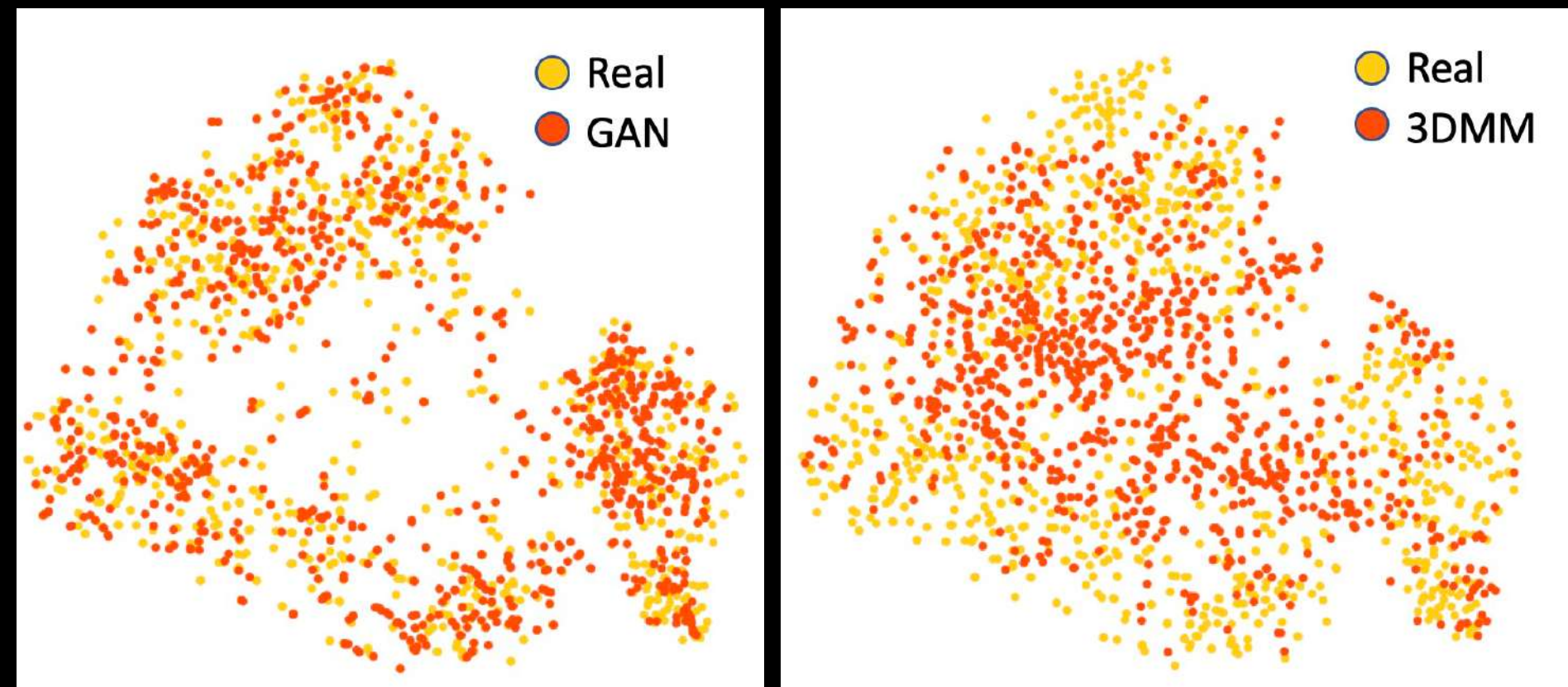
Synthesizing Expressions



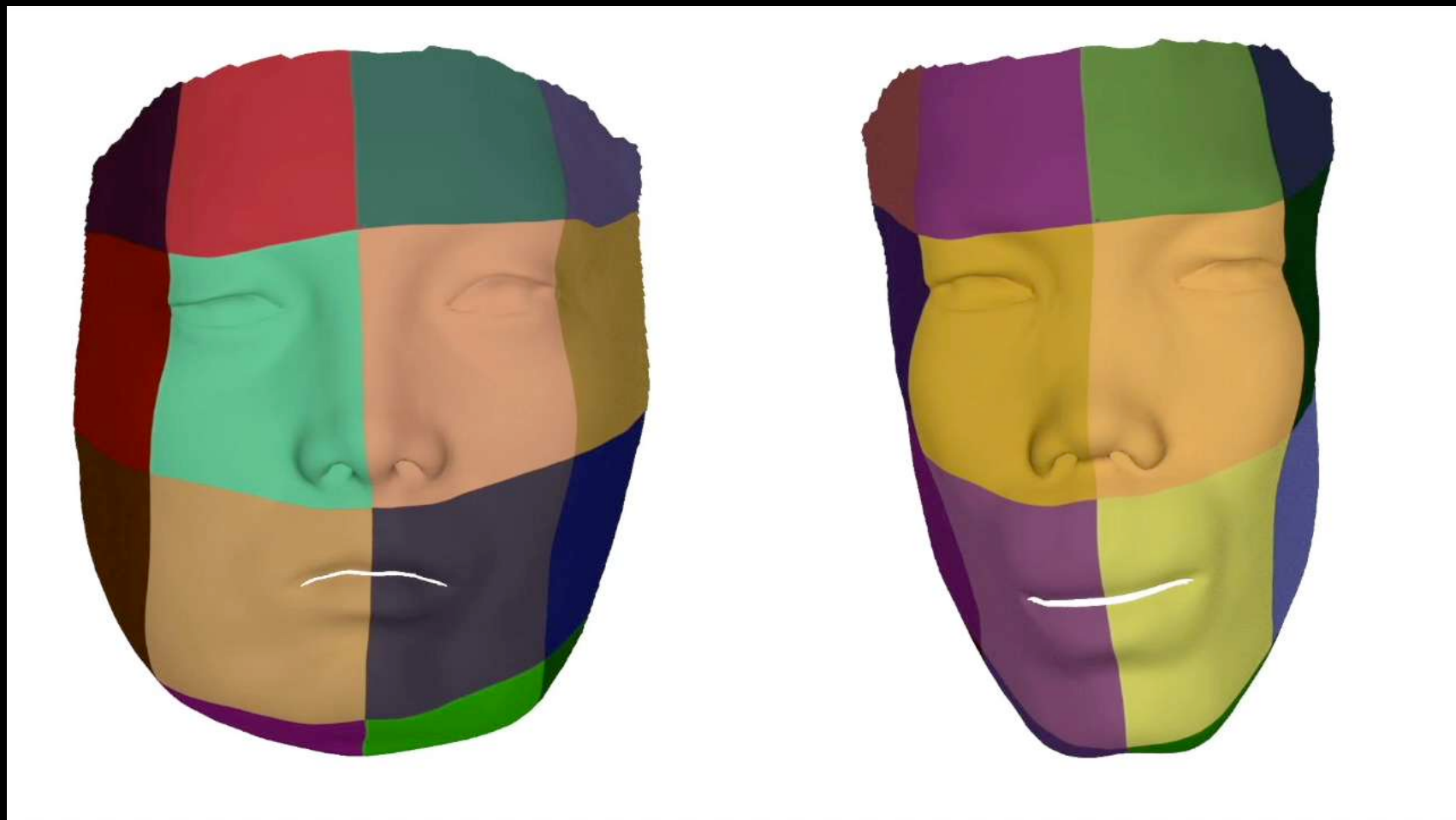


Shamai, Slossberg, K. 2018/2019 Synthesizing photometries and geometries with GANs & 

2D embedding identities



Training iterations (GAN)



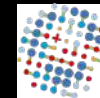


ISRAEL
SCIENCE
FOUNDATION



Ministry of Science,
Technology and Space

SCHMIDT FUTURES



The Lokey Center

Artificial Intelligence Algorithms to Assess Hormonal Status From Tissue Microarrays in Patients With Breast Cancer

Gil Shamai Yoav Binenbaum Ron Slossberg



Irit Duek



Ziv Gil



Ron Kimmel

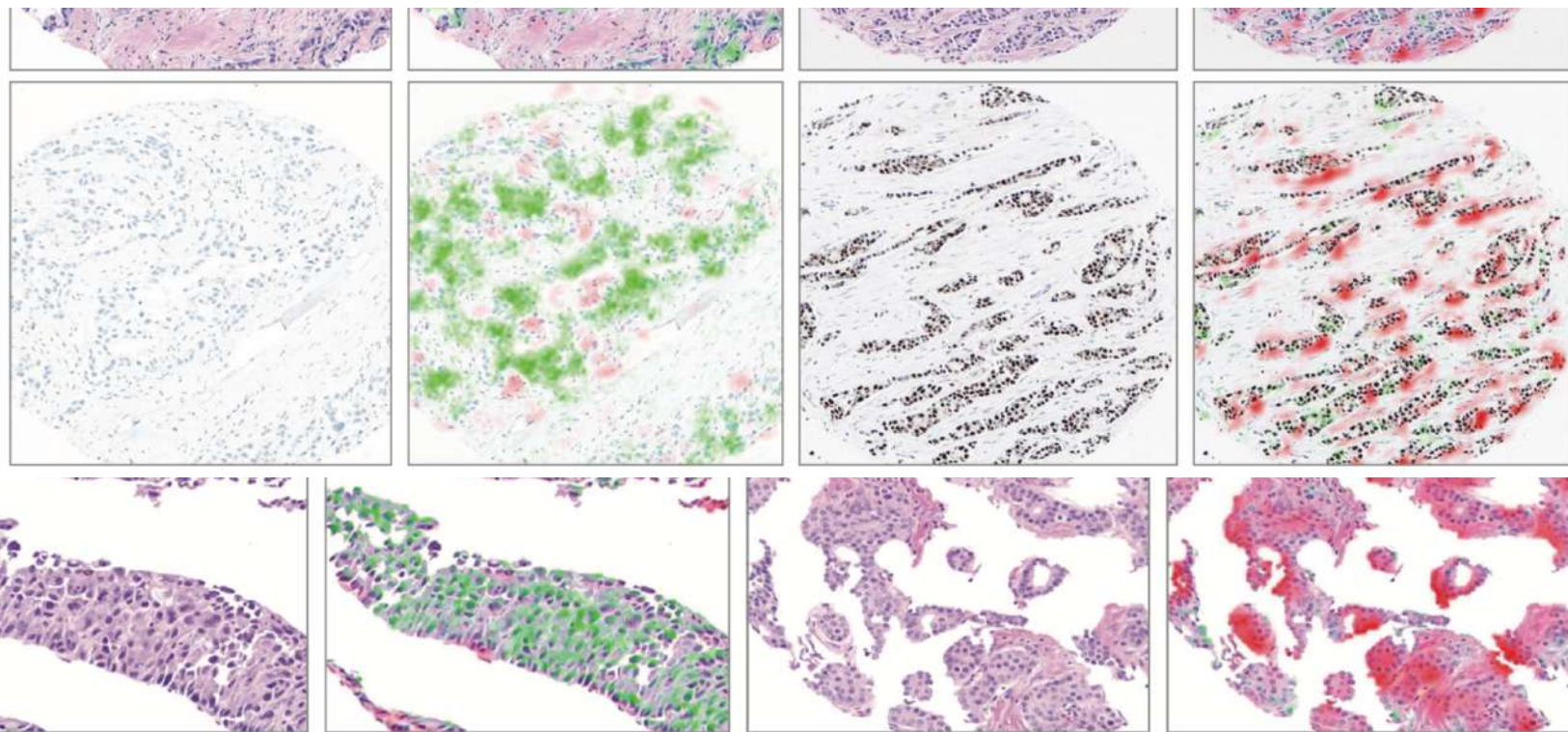


Geometric Image Processing lab

Original Investigation | Oncology

Artificial Intelligence Algorithms to Assess Hormonal Status From Tissue Microarrays in Patients With Breast Cancer

Gil Shamai, MSc; Yoav Binenbaum, MD, PhD; Ron Slossberg, MSc; Irit Duek, MD; Ziv Gil, MD, PhD; Ron Kimmel, DSc

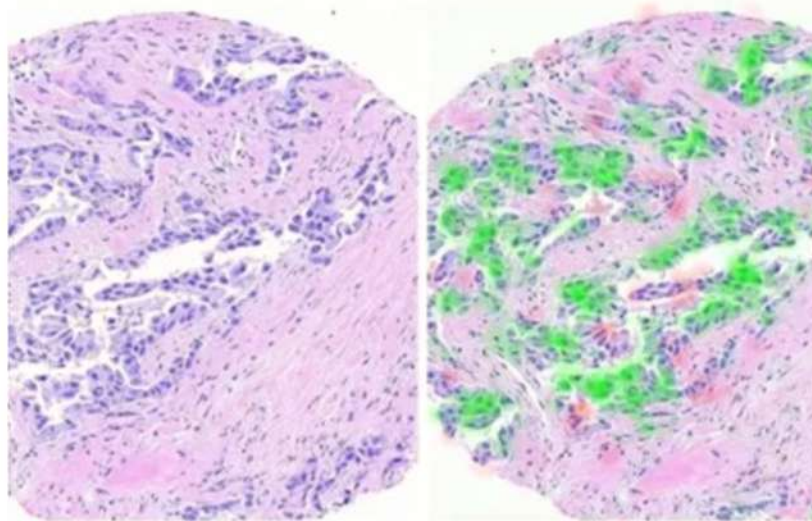




GROUNDBREAKING AI-BASED CANCER TREATMENT DEVELOPED BY ISRAELI RESEARCHERS

2 minute read.

By LEON SVERDLOV



The original scan (left) and the areas where information was extracted (in red and green, right) using the technology developed at the Technion (photo credit: TECHNION SPOKESPERSON'S OFFICE)

The new technology allows AI to identify molecular features of cancer

www.news.cn
新华网
NEWS
www.xinhuanet.com

Israeli research technology to i

Source: Xinhua | 2019-08-19 22:22



JERUSALEM, Aug. 19 (Xinhua) — Deep learning (DL) technology that is being developed at the northern Israel Insti

This is a method for breast cancer patients

The new method, based on hematoxylin and taken in a biopsy

This staining a

edge

Free release Privately funded Control us

Win triple fees back

RE WORLD NIGERIA OPIN

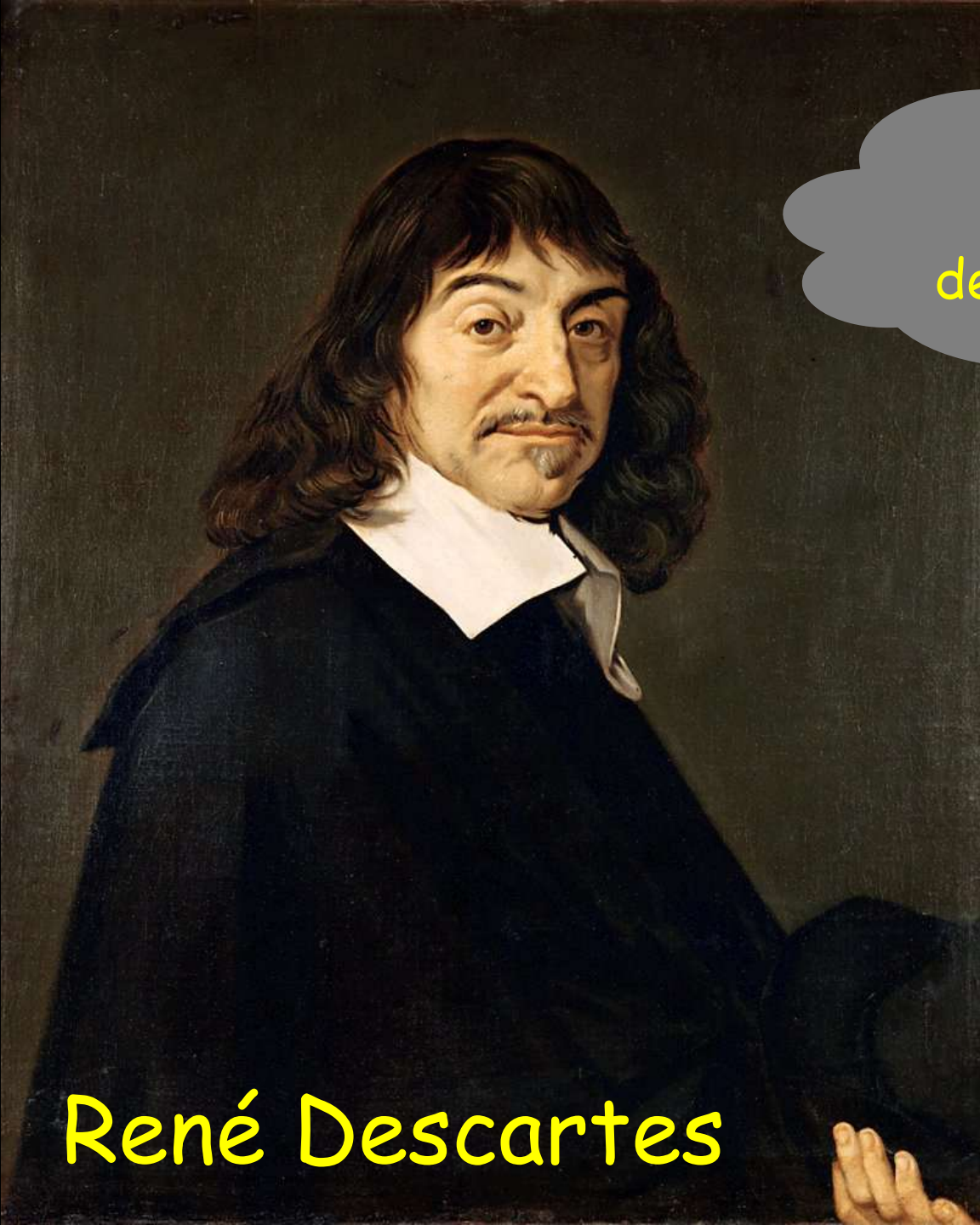
o-learning treatments

ology that is expected to te of Technology

ges of breast cancer

hematoxylin and

טכנולוגיה
סלוסברג מ
בטיפול בגין

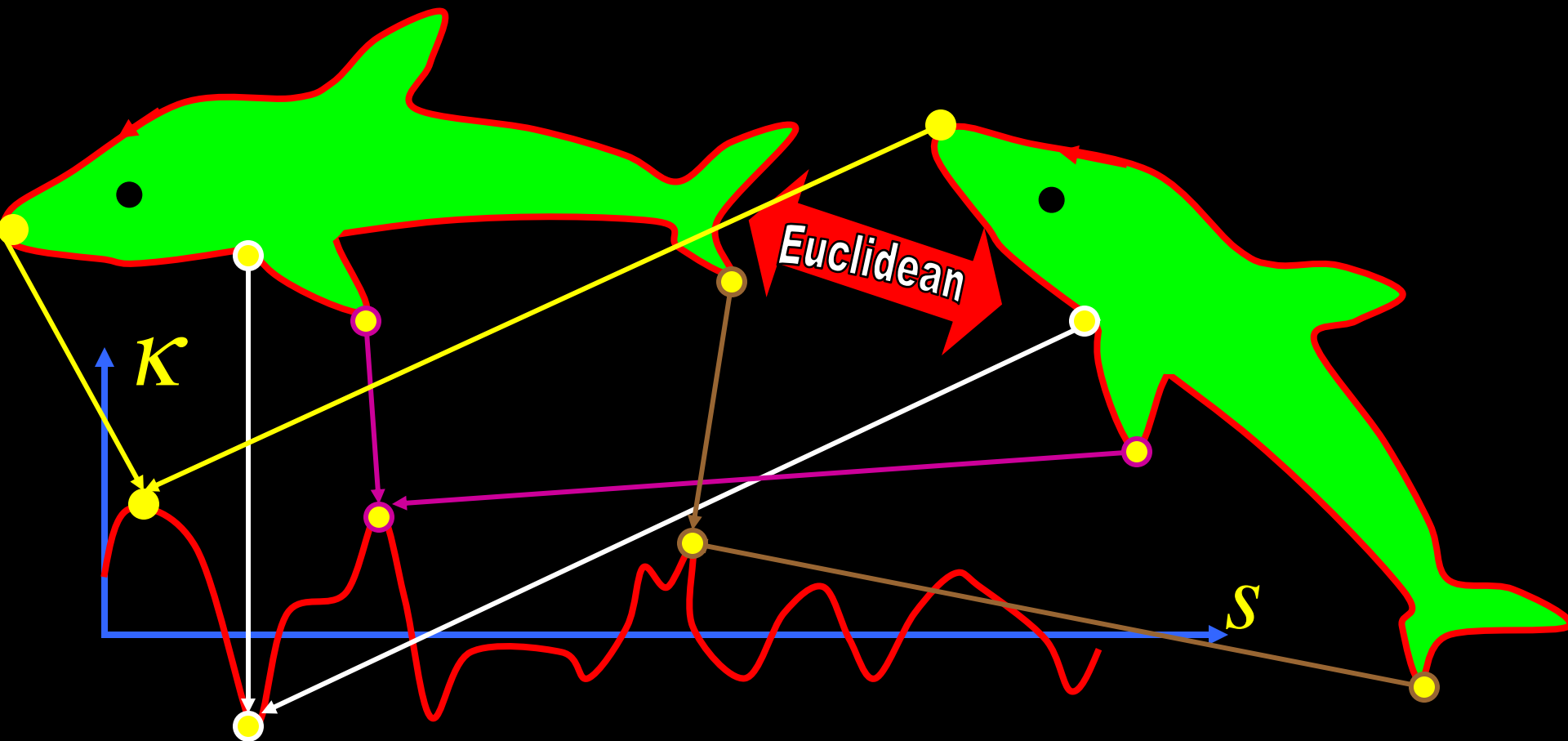
A portrait painting of René Descartes, a French philosopher, mathematician, and scientist. He has long, wavy brown hair and a mustache. He is wearing a dark robe over a white collared shirt. A thought bubble originates from his head.

How could we
use algebra to
describe geometry?

René Descartes

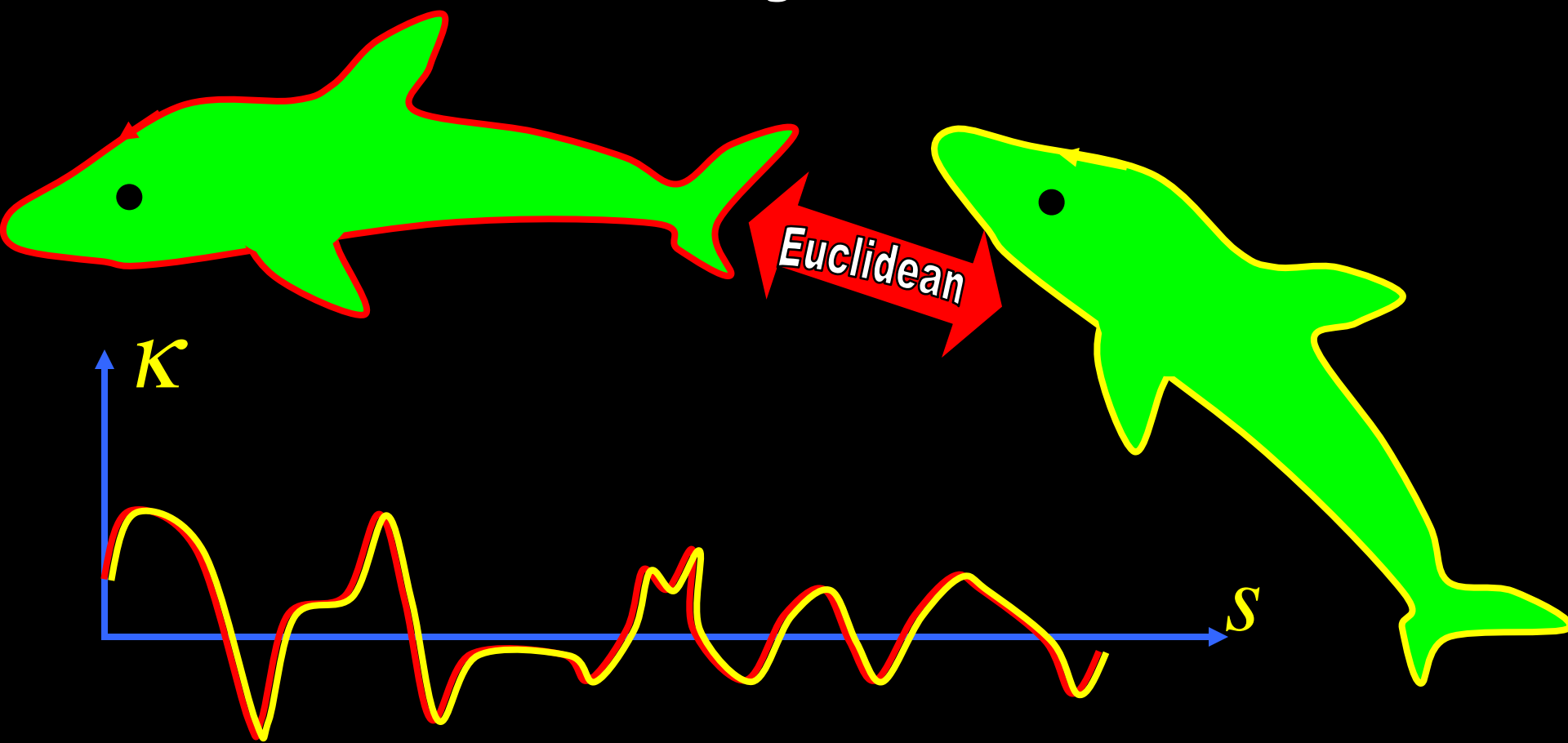
Differential Signatures

- Euclidean invariant signature $\{s, K(s)\}$

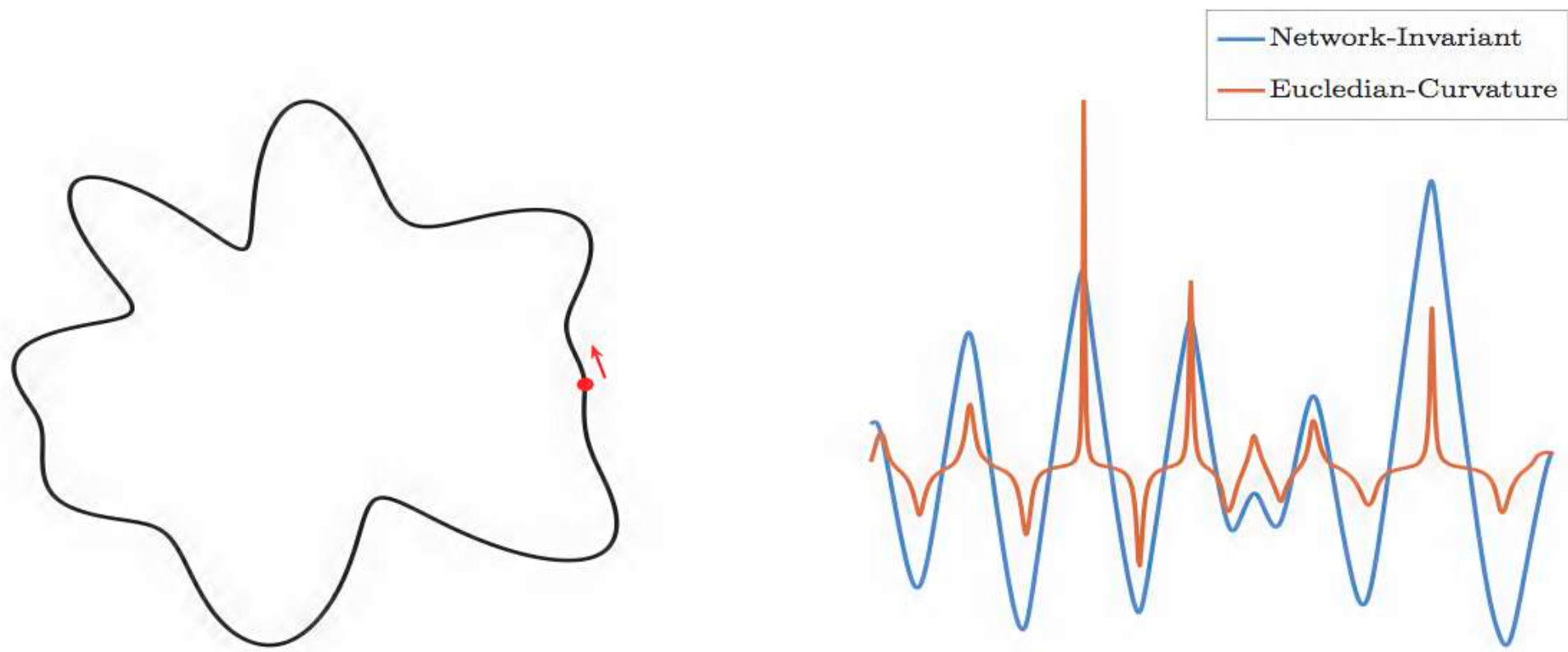


Differential Signatures

- Euclidean invariant signature $\{s, K(s)\}$



Learning invariants



Deep Eikonal solvers

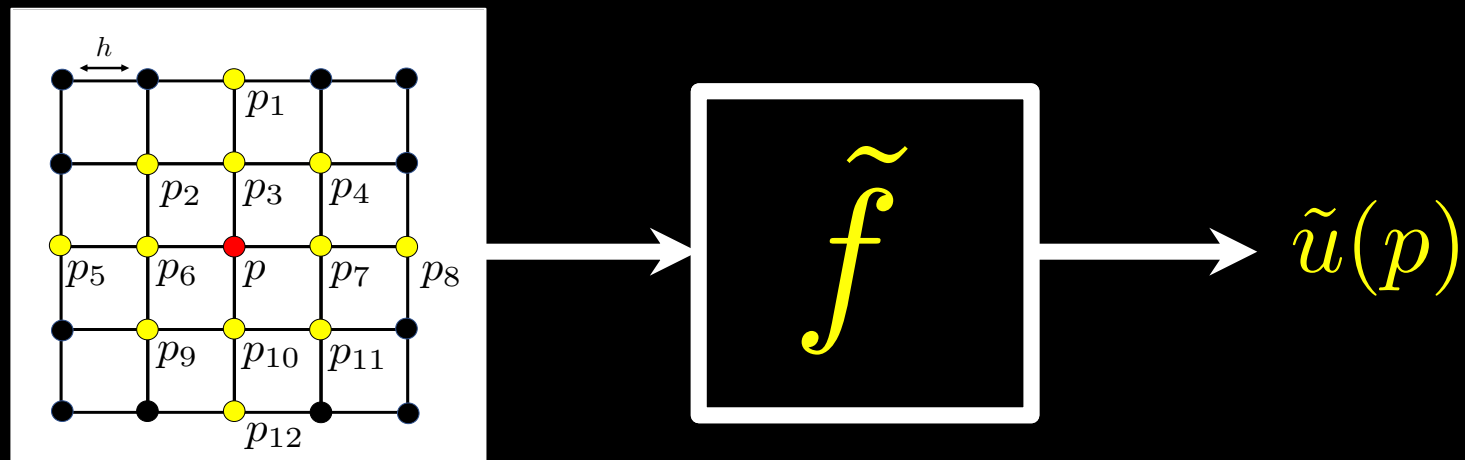
$$|\nabla u(x)| = 1, \quad x \in \Omega \setminus \Gamma$$

$$u(x) = 0, \quad x \in \Gamma$$

Local numerical approximations using neural networks

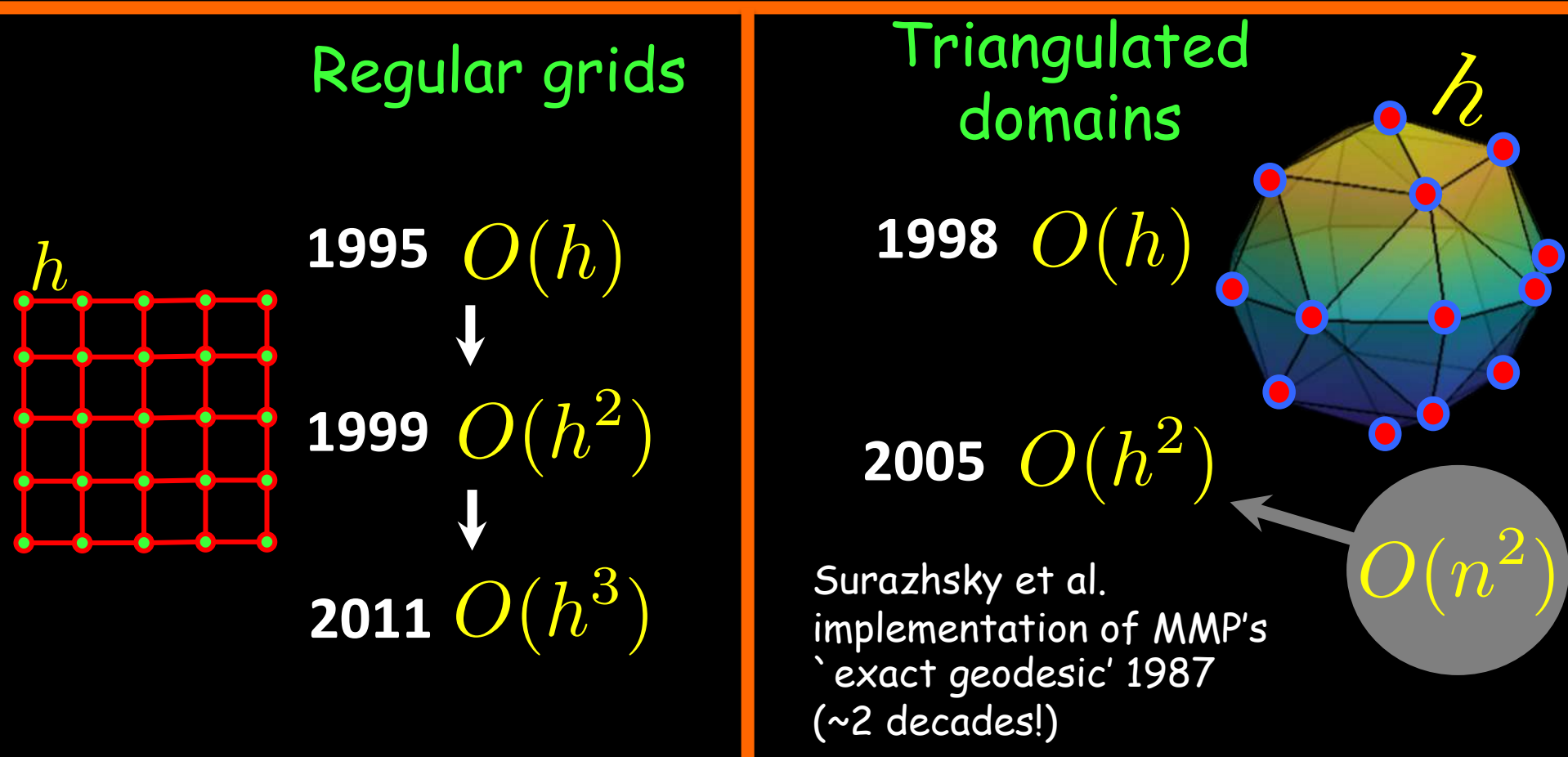
Easy to extend the support

Approximation is learned from analytically known solutions

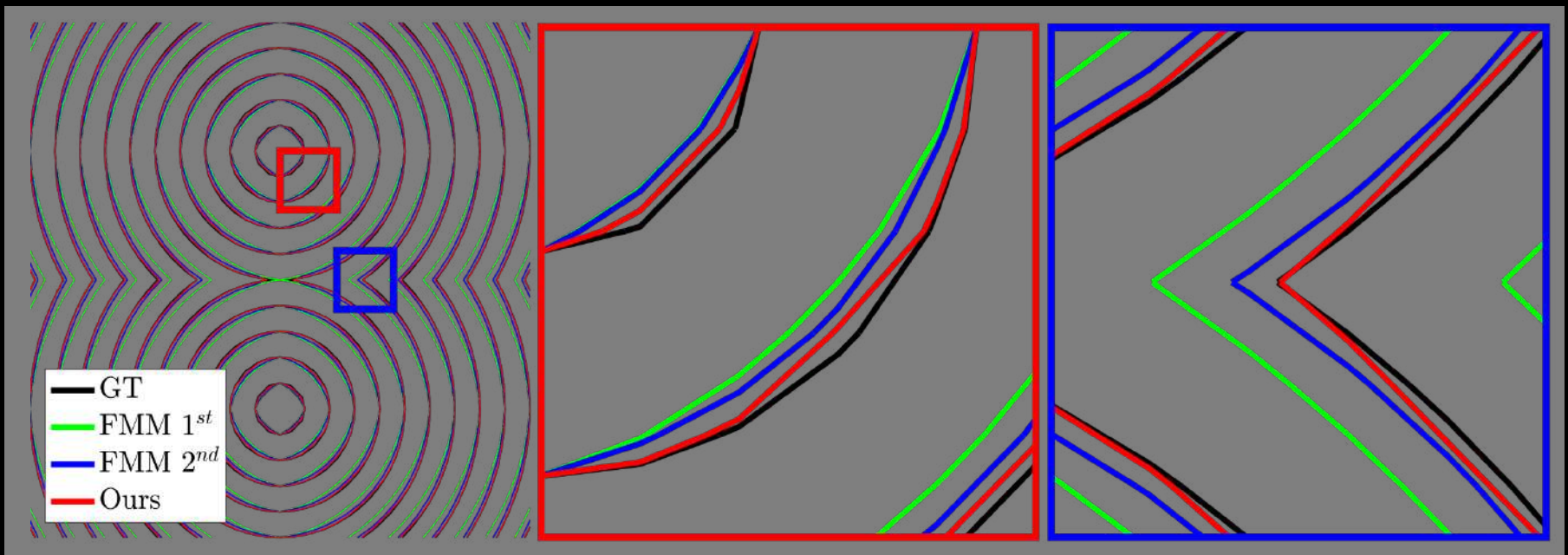


On the evolution of accuracy/complexity

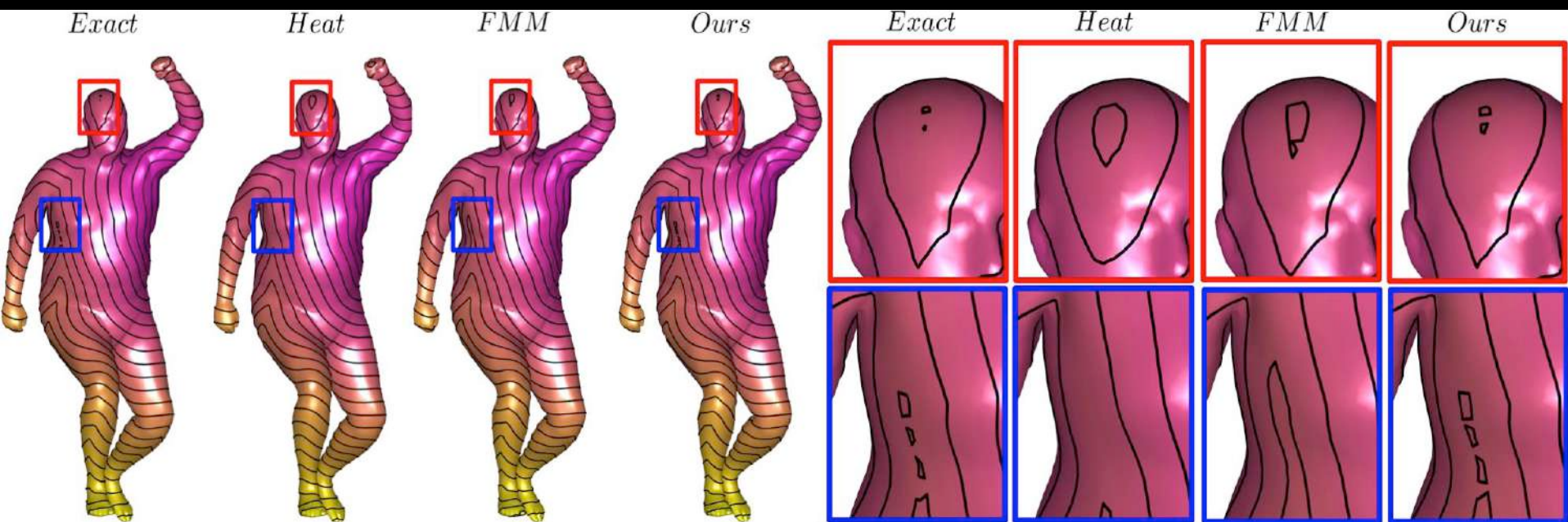
- Fast Marching (quasi-linear complexity) $\sim O(n)$



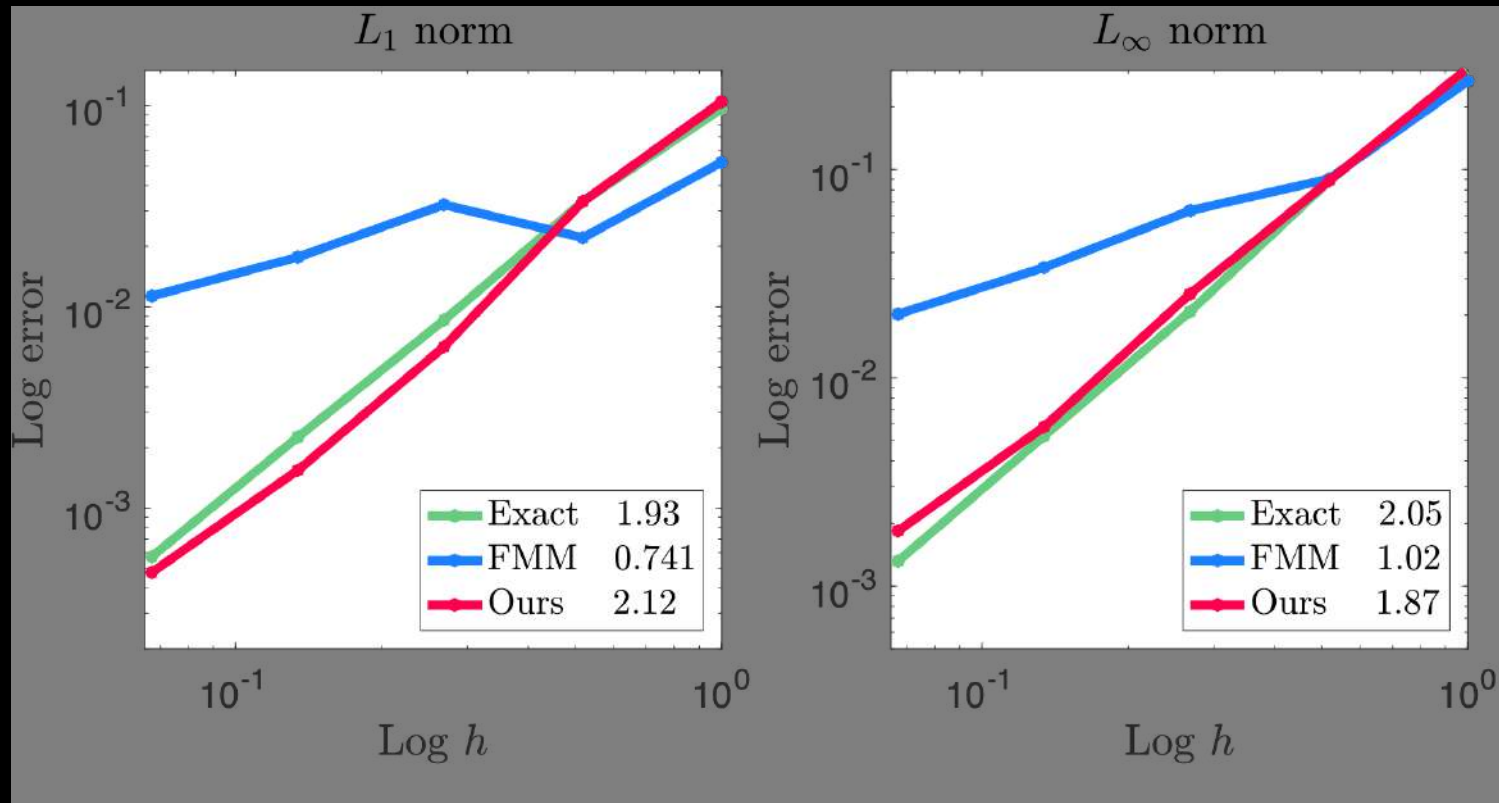
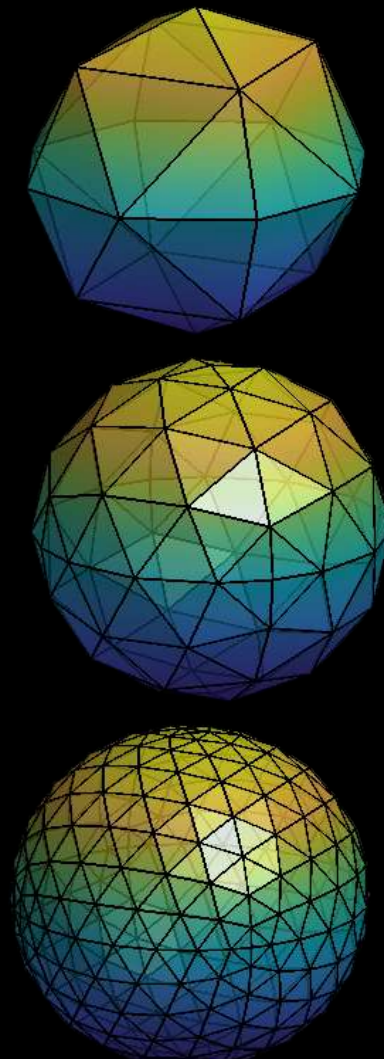
Results for Cartesian grids



Inter-dataset generalization



Order of accuracy



Momenet

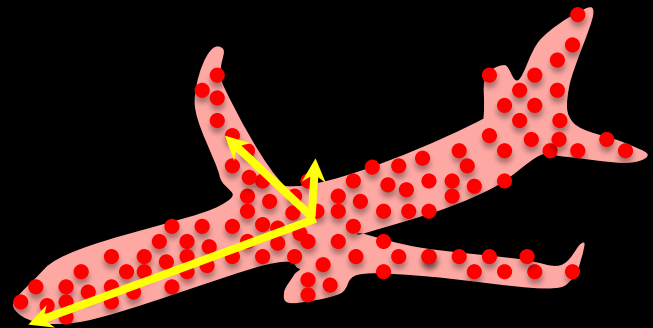


Geometric moments

Given a set of points $P \subset \mathbb{R}^3$ and $p_i = (x_i, y_i, z_i)^T \in P$

$$1^{\text{st}} \text{ moments} \quad \bar{p} = (\bar{x}, \bar{y}, \bar{z})^T = \frac{1}{n} \sum_{i=1}^n p_i$$

$$2^{\text{nd}} \text{ moments} \quad \frac{1}{n} \sum_{i=1}^n p_i p_i^T$$



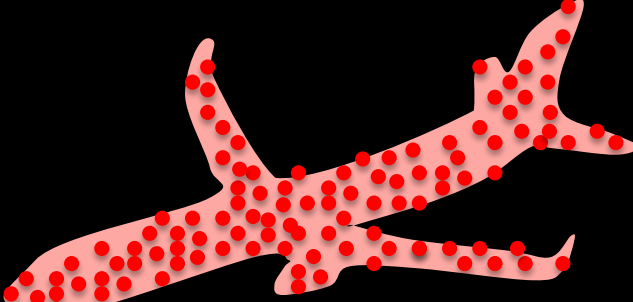
Young. The algebra of invariants, 1903

Hall. Three-dimensional moment invariants. PAMI, 1980

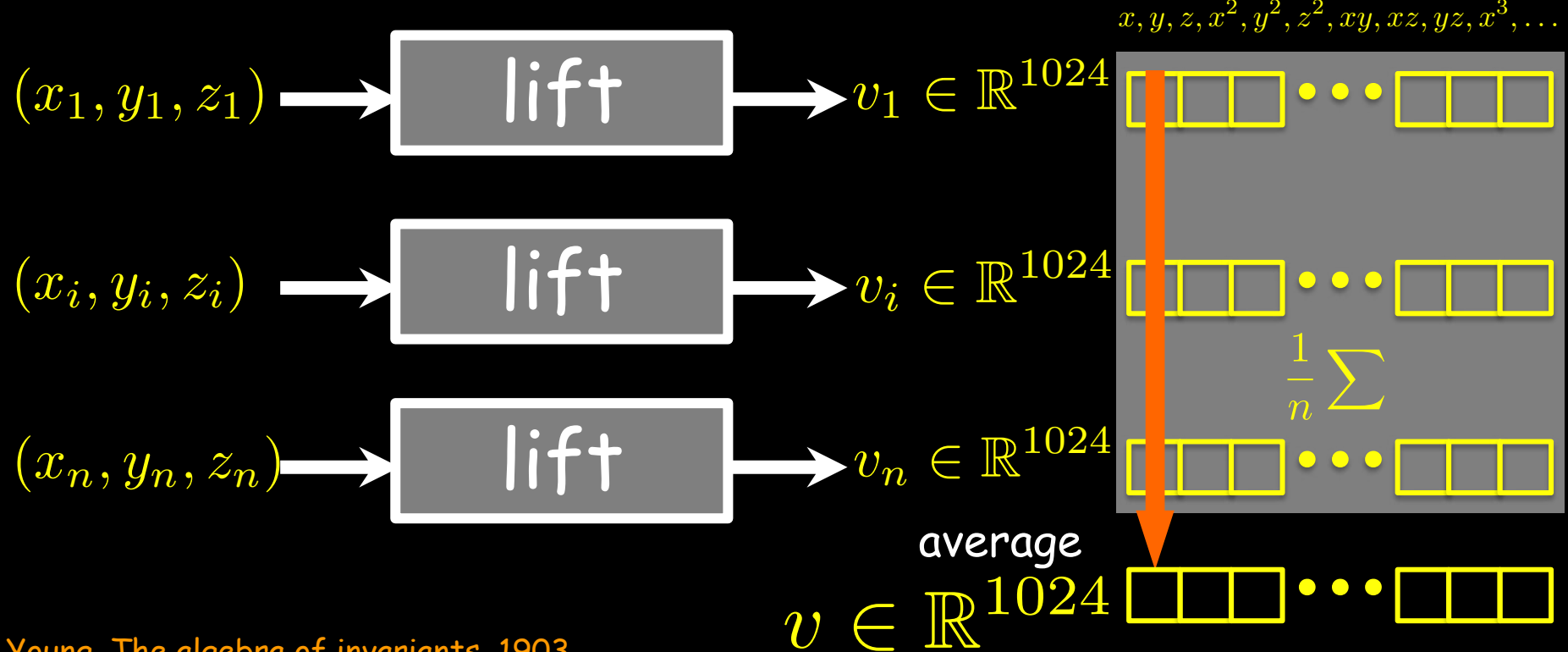
Maxwell, Learning, invariance, and generalization in high-order neural networks. Applied optics, 1987

Su, Mo, Guibas. Pointnet: Deep learning on point sets. CVPR'17

Joseph-Rivlin, Zvirin, K., GMDL workshop, ICCV'19



Moments



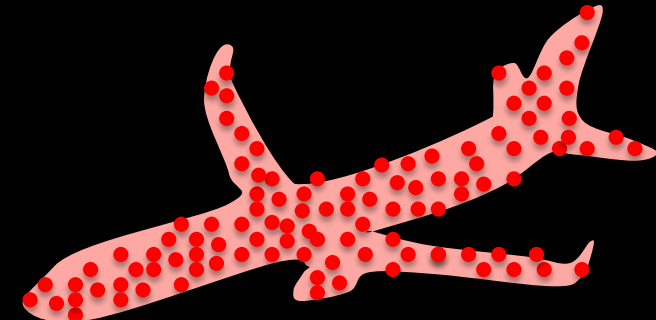
Young. The algebra of invariants, 1903

Hall. Three-dimensional moment invariants. PAMI, 1980

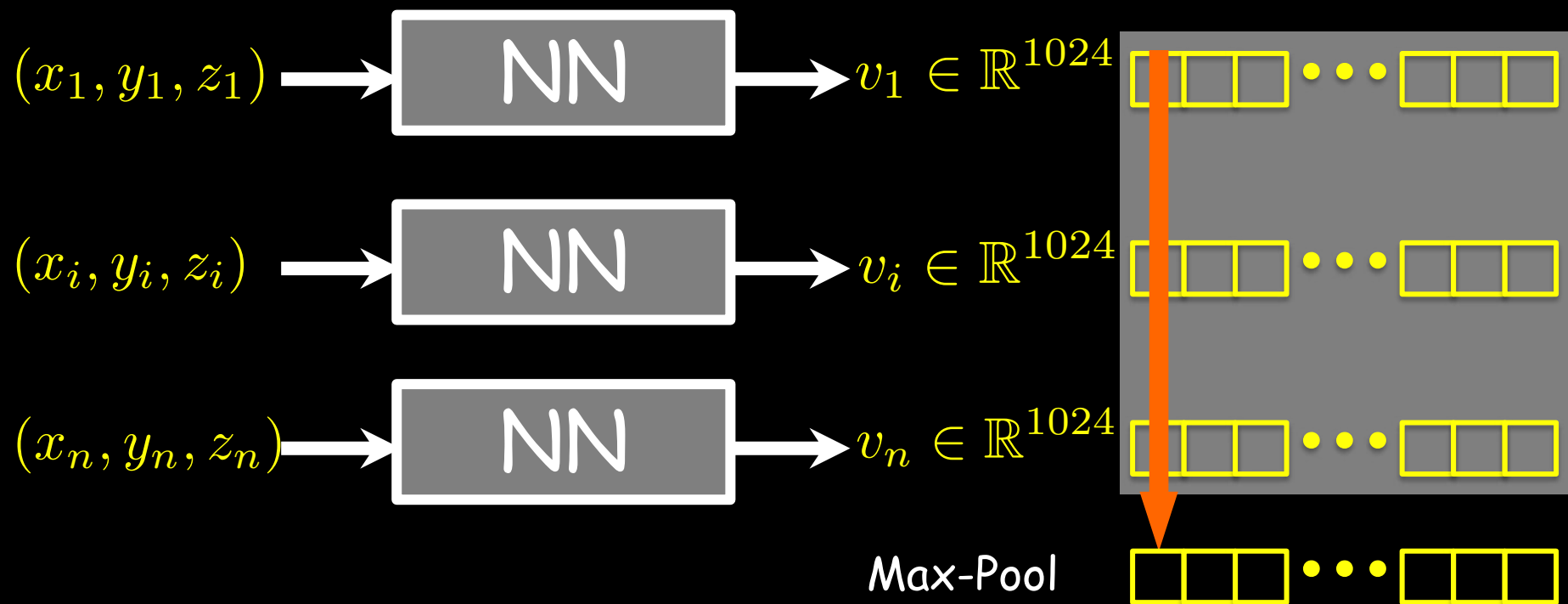
Maxwell, Learning, invariance, and generalization in high-order neural networks. Applied optics, 1987

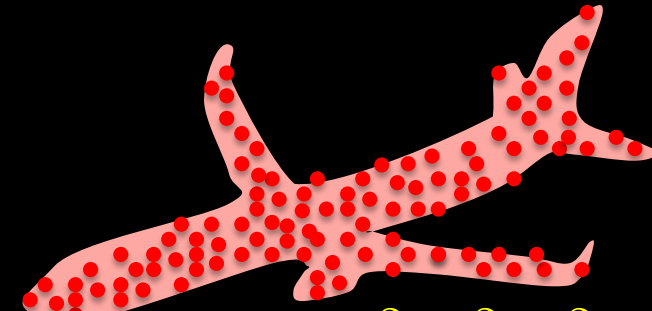
Su, Mo, Guibas. Pointnet: Deep learning on point sets. CVPR'17

Joseph-Rivlin, Zvirin, K., GMDL workshop, ICCV'19



PointNet





Momenet

$$(x_1, y_1, z_1, x_1^2, y_1^2, z_1^2, x_1y_1, x_1z_1, y_1z_1)$$

$$(x_1, y_1, z_1) \rightarrow \text{NN} \rightarrow v_1 \in \mathbb{R}^{1024}$$

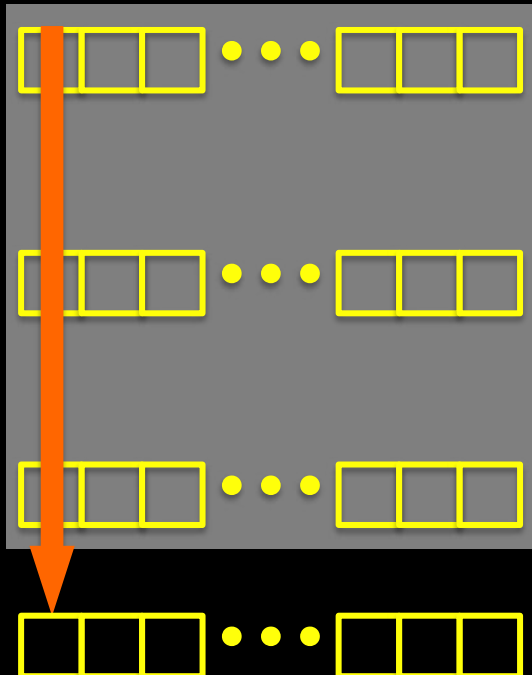
$$(x_i, y_i, z_i, x_i^2, y_i^2, z_i^2, x_iy_i, x_iz_i, y_iz_i)$$

$$(x_i, y_i, z_i) \rightarrow \text{NN} \rightarrow v_i \in \mathbb{R}^{1024}$$

$$(x_n, y_n, z_n, x_n^2, y_n^2, z_n^2, x_ny_n, x_nz_n, y_nz_n)$$

$$(x_n, y_n, z_n) \rightarrow \text{NN} \rightarrow v_n \in \mathbb{R}^{1024}$$

Max-Pool



Results on ModelNet40

	Memory (MB)	Inference Time (msec)	Overall Accuracy (%)
PointNet	40	5.6	89.2
PointNet(baseline)	20	5.1	87.9
Momen ^e t	20	5.1	89.6
PointNet++	12	10.4	90.7
DGCNN	21	17.3	92.2
PCNN	17	54.1	92.3
Momen ^e t (+kNN)	21	9.6	92.4

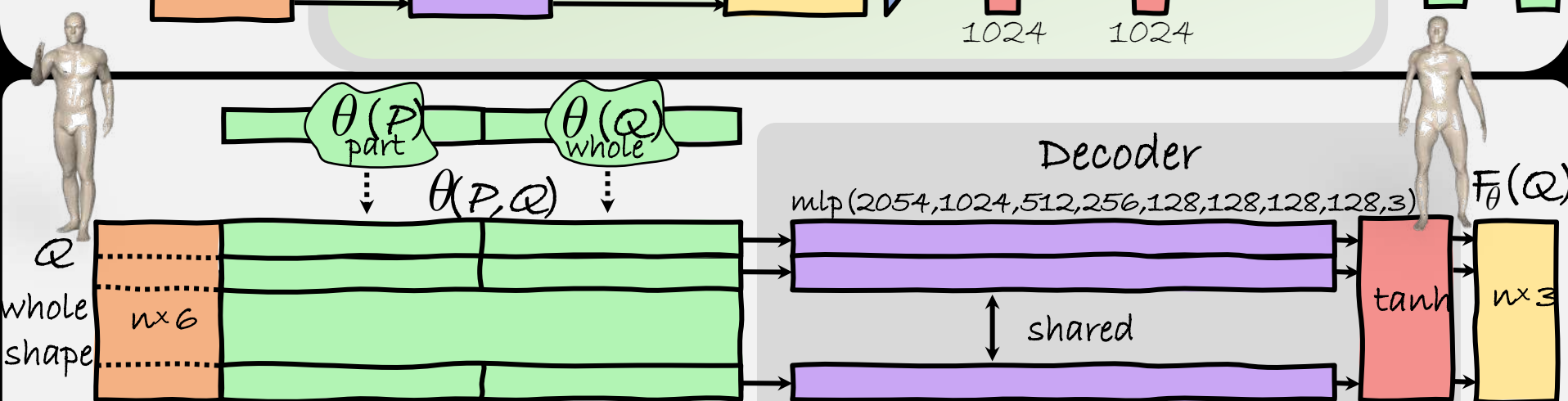
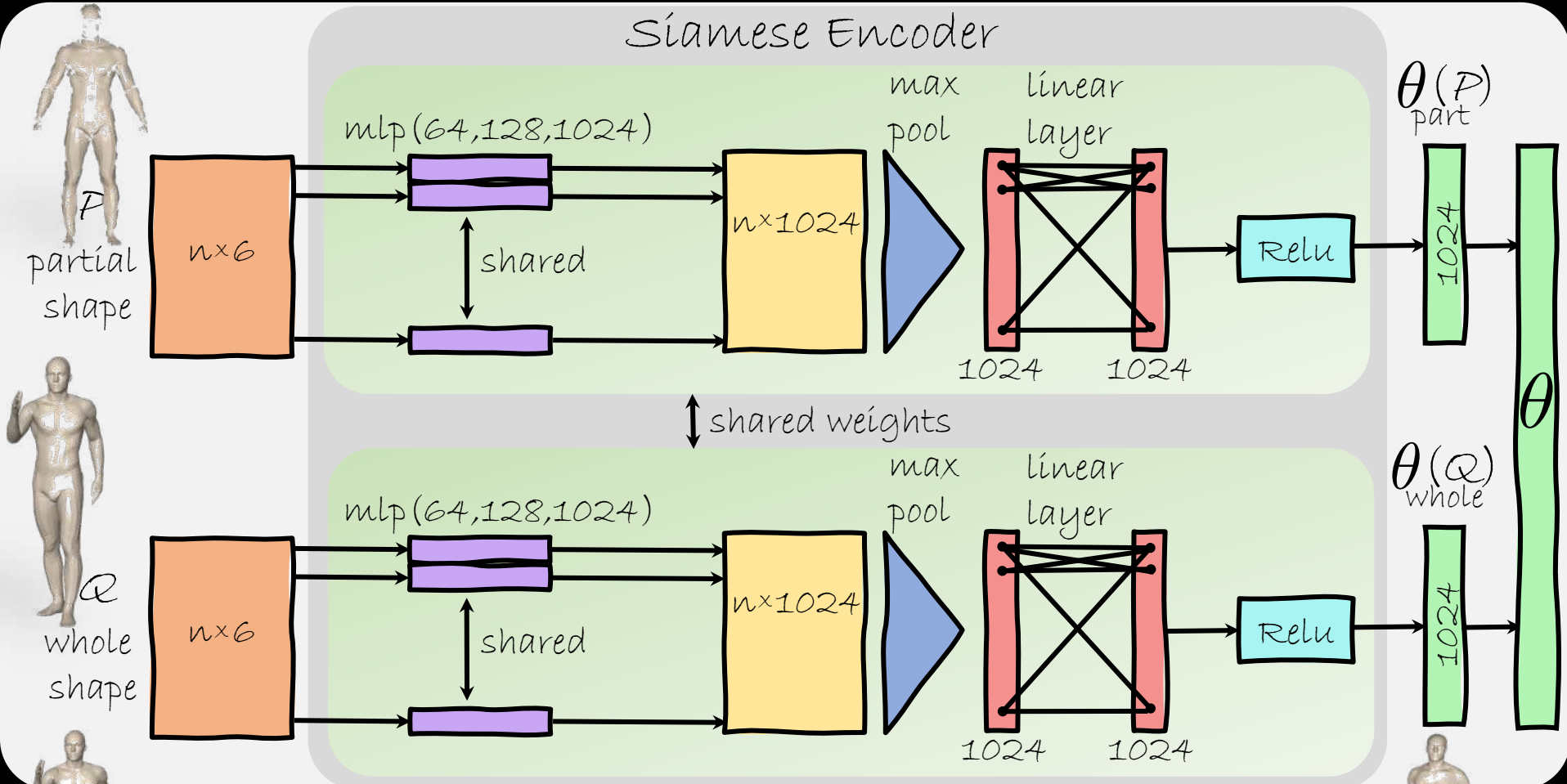
Wu, et al.. 3D shapenets. CVPR2015.

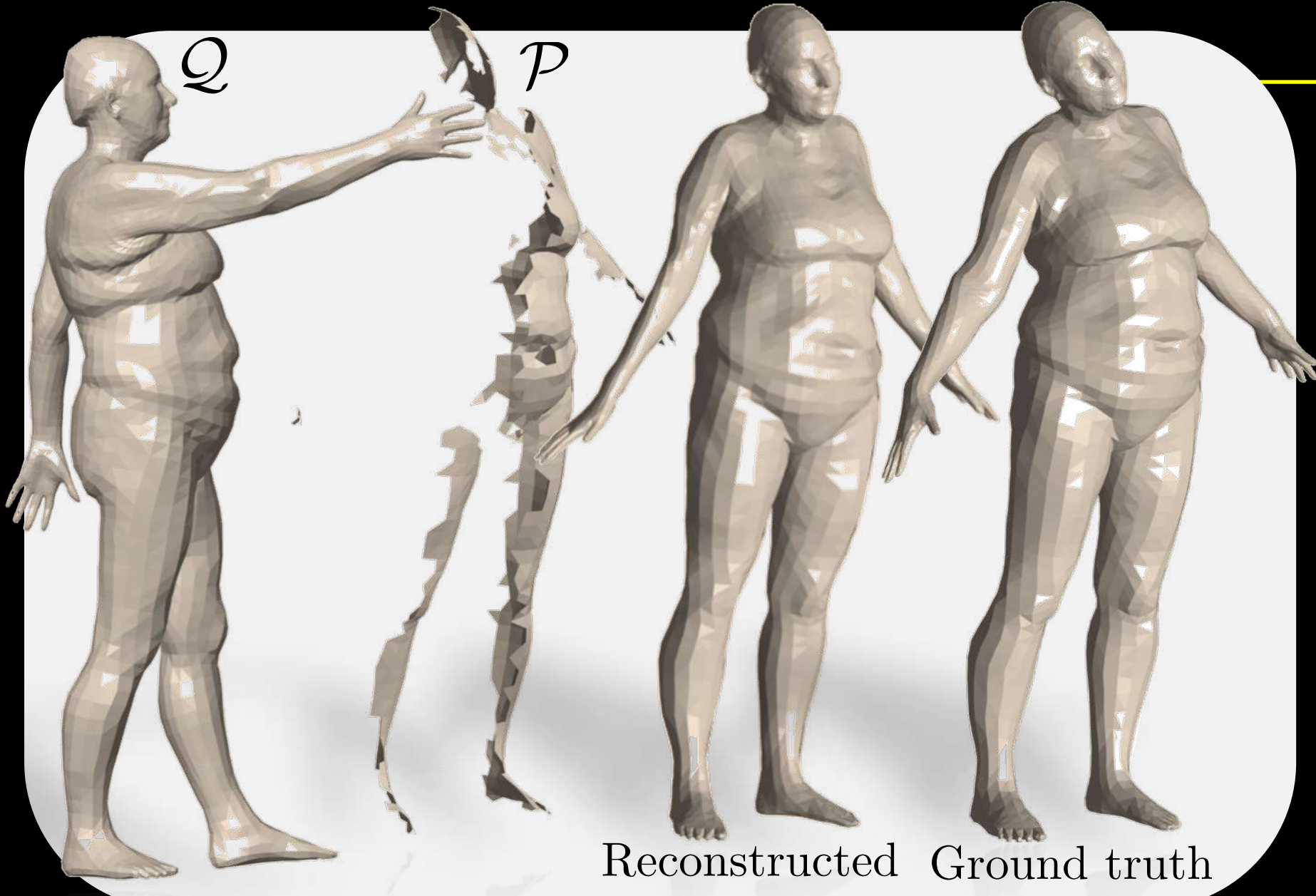
Wang et al. . Dynamic graph CNN. Arxiv 2018.

Atzmon, Maron, & Lipman. Point convolutional NN. ACM T Graph. 2018

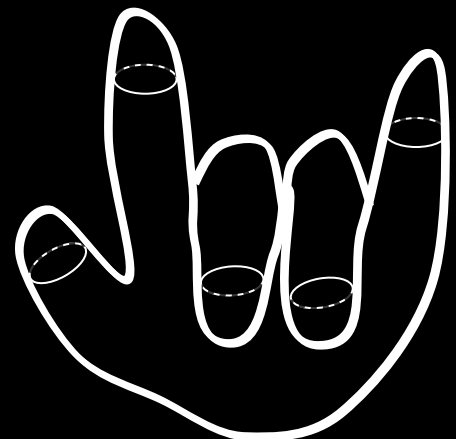
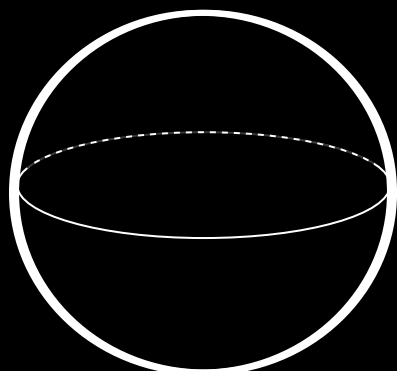
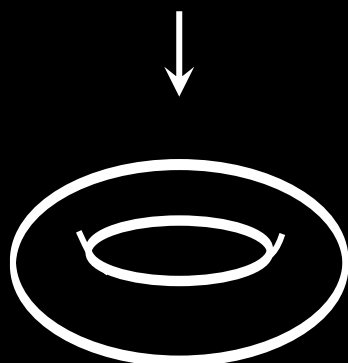
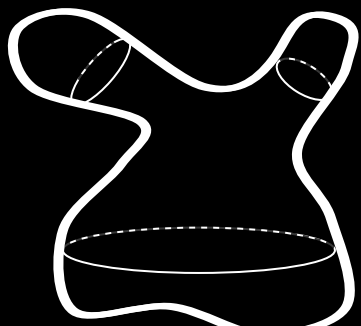
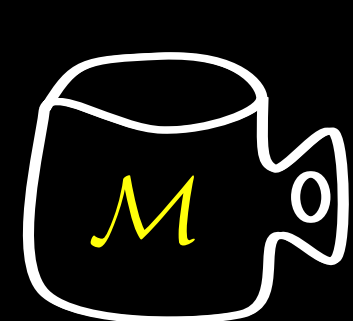
Joseph-Rivlin, Zvirin, K., Flavor the moments, GMDL workshop, ICCV'19

Siamese Encoder





Manifold vs. Riemannian Manifold



↓
 \sim
iso

Shapes as metric spaces

$$d_{GH}(\text{Hand}, \text{Hand}) < d_{GH}(\text{Hand}, \text{Foot})$$

*MDS, GMDS, SGMDs, GDD, PCA, RPCA,
F-Maps, FM-Net, GMDS-Net, SF-Maps*

Functional Maps

Ovsjanikov et al. 2012



$$\{\psi_i\}$$

$$f = \sum_i \langle f, \psi_i \rangle \psi_i = \sum_i \alpha_i \psi_i$$



$$\{\phi_i\}$$

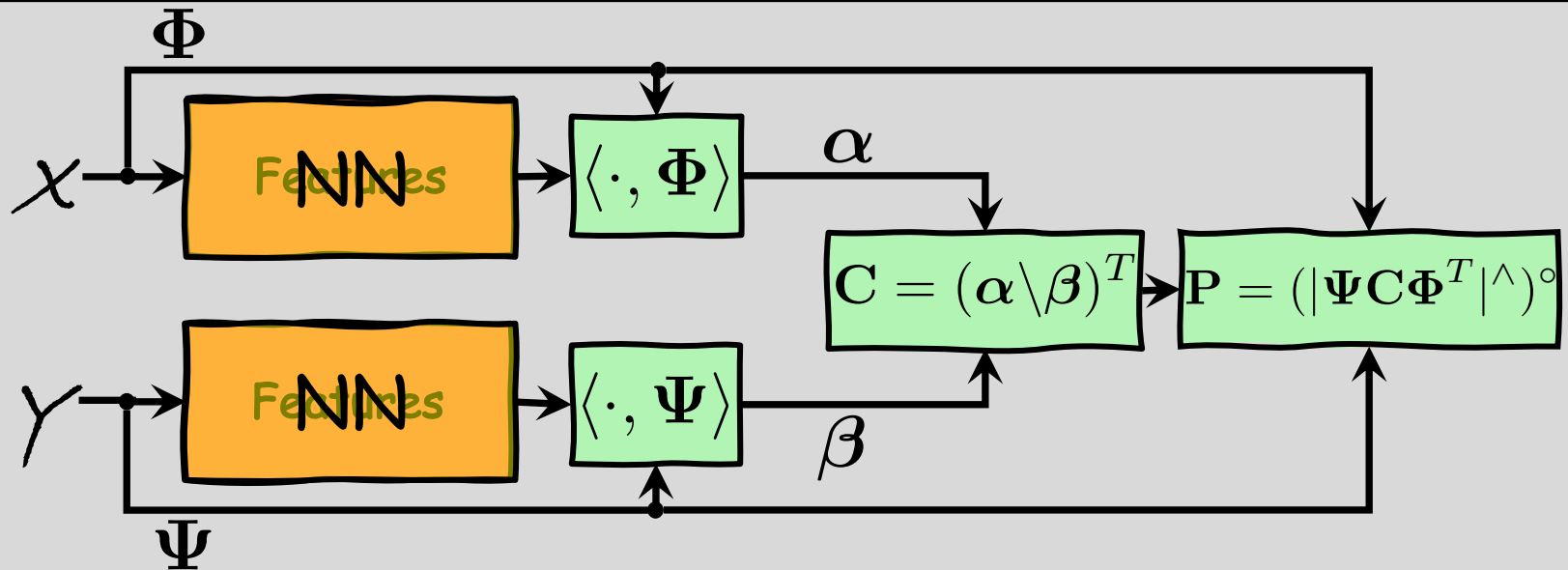
$$f = \sum_i \langle f, \phi_i \rangle \phi_i = \sum_i \beta_i \phi_i$$

$$\beta = C\alpha$$

$$C_{ij} = \langle T(\phi_i), \psi_j \rangle$$

Functional Maps

$$\mathcal{Y} \approx P\mathcal{X}$$



Ovsjanikov et al. 2012

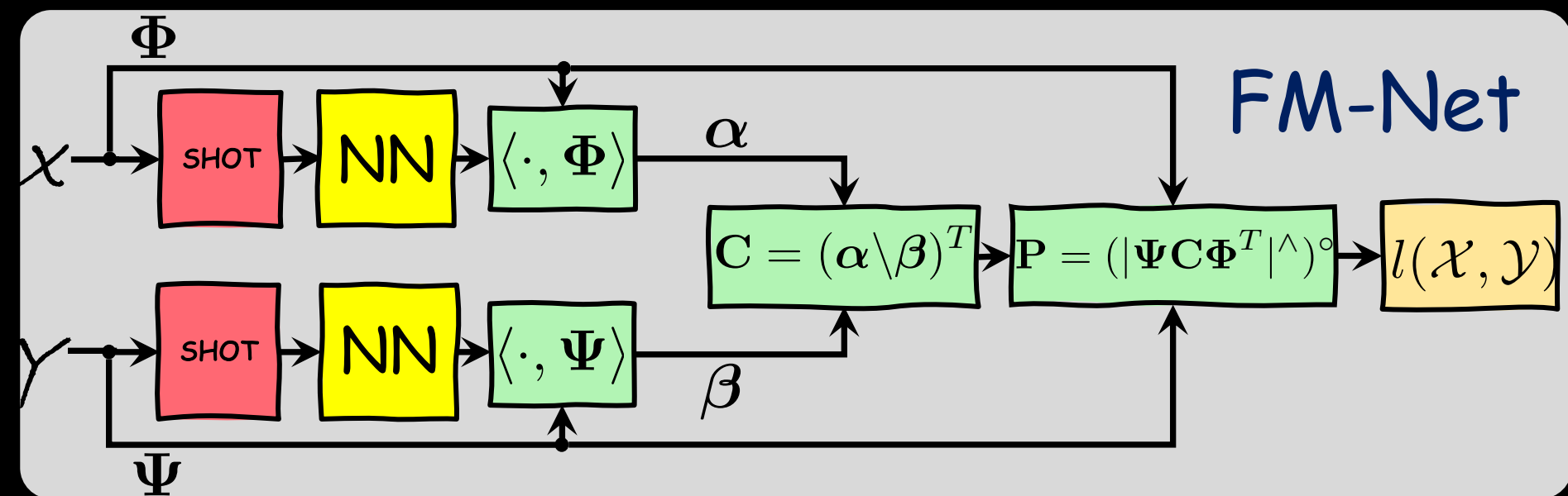
Litany, Remez, Rodola, A Bronstein, M Bronstein ICCV'17

Halimi, Litany, Rodolà, Bronstein, K. CVPR'19

Roufosse, Sharma, Ovsjanikov, ICCV'19

Functional Maps-Net

$$l_{sup}(\mathcal{X}, \mathcal{Y}) = \sum_{i \in \mathcal{X}} \sum_{j \in \mathcal{Y}} p_{ij} d_{\mathcal{Y}}^2(j, \pi^*(i))$$



Ovsjanikov et al. 2012

Litany, Remez, Rodola, A Bronstein, M Bronstein ICCV'17

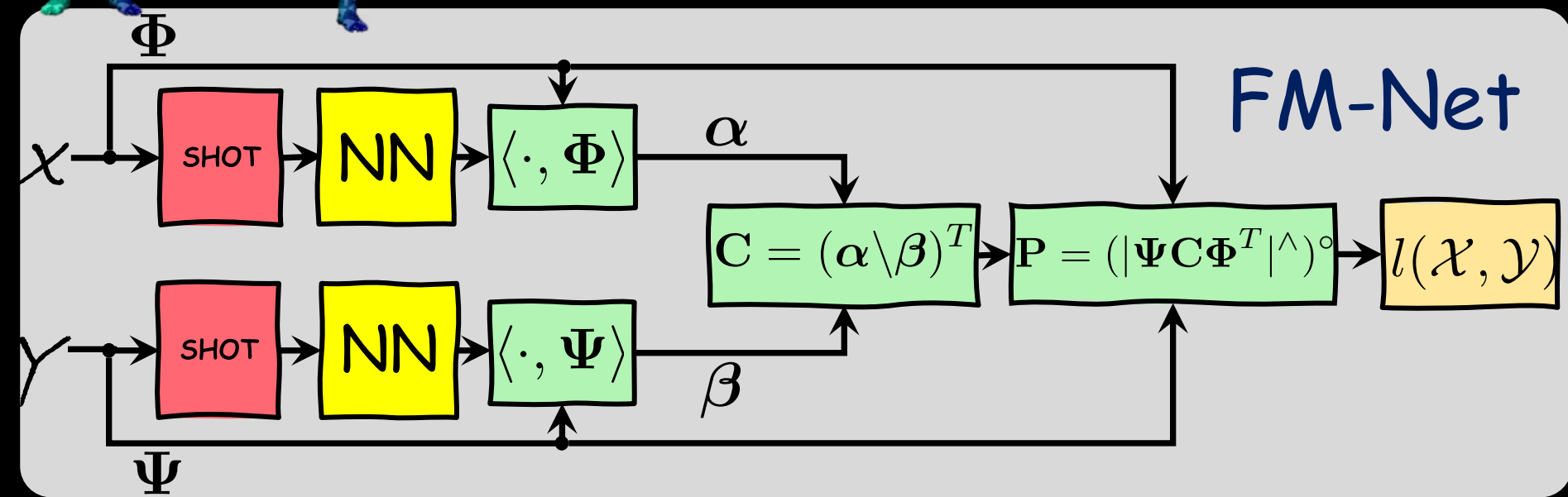
Halimi, Litany, Rodolà, Bronstein, K. CVPR'19

Roufosse, Sharma, Ovsjanikov, ICCV'19



Unsupervised Functional Maps-Net

$$l_{uns}(\mathcal{X}, \mathcal{Y}) = \|D_{\mathcal{X}} - P D_{\mathcal{Y}} P^T\|$$



Ovsjanikov et al. 2012

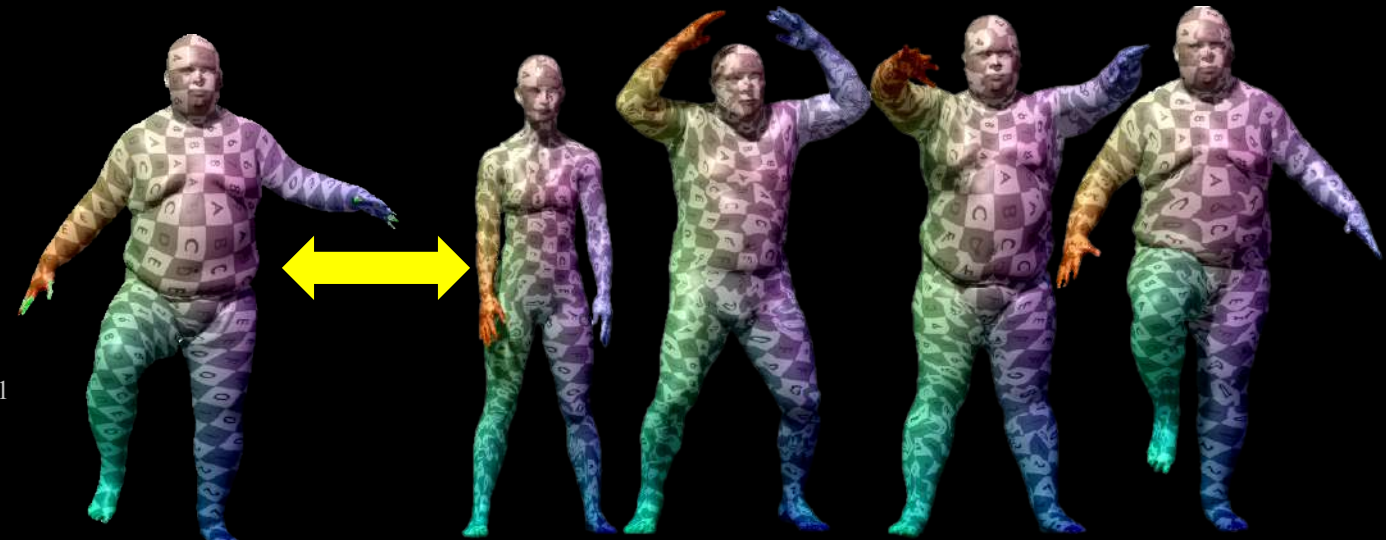
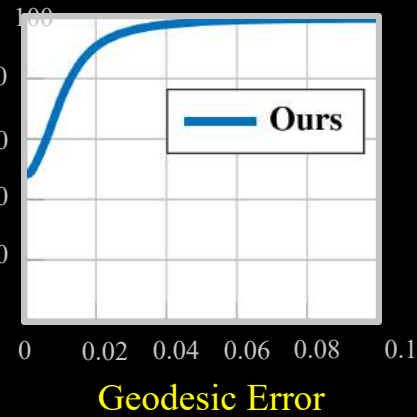
Litany, Remez, Rodola, A Bronstein, M Bronstein ICCV'17

Halimi, Litany, Rodolà, Bronstein, K. CVPR'19

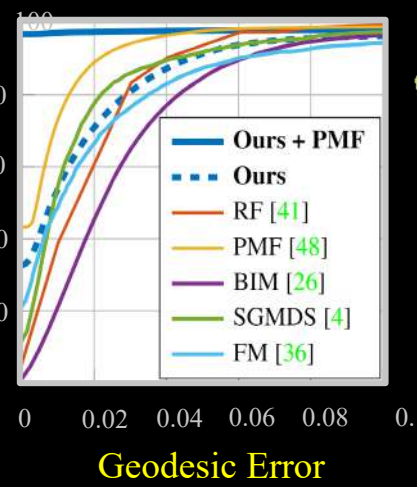
Roufosse, Sharma, Ovsjanikov, ICCV'19

Generalization

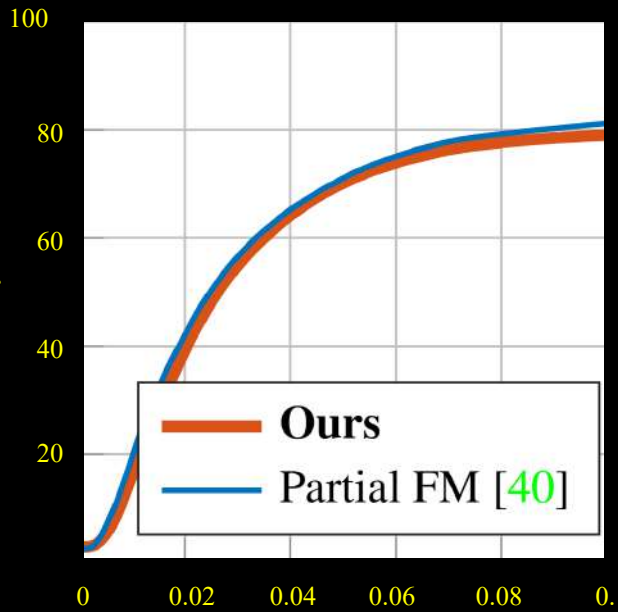
%Correspondence



%Correspondence



%Correspondence

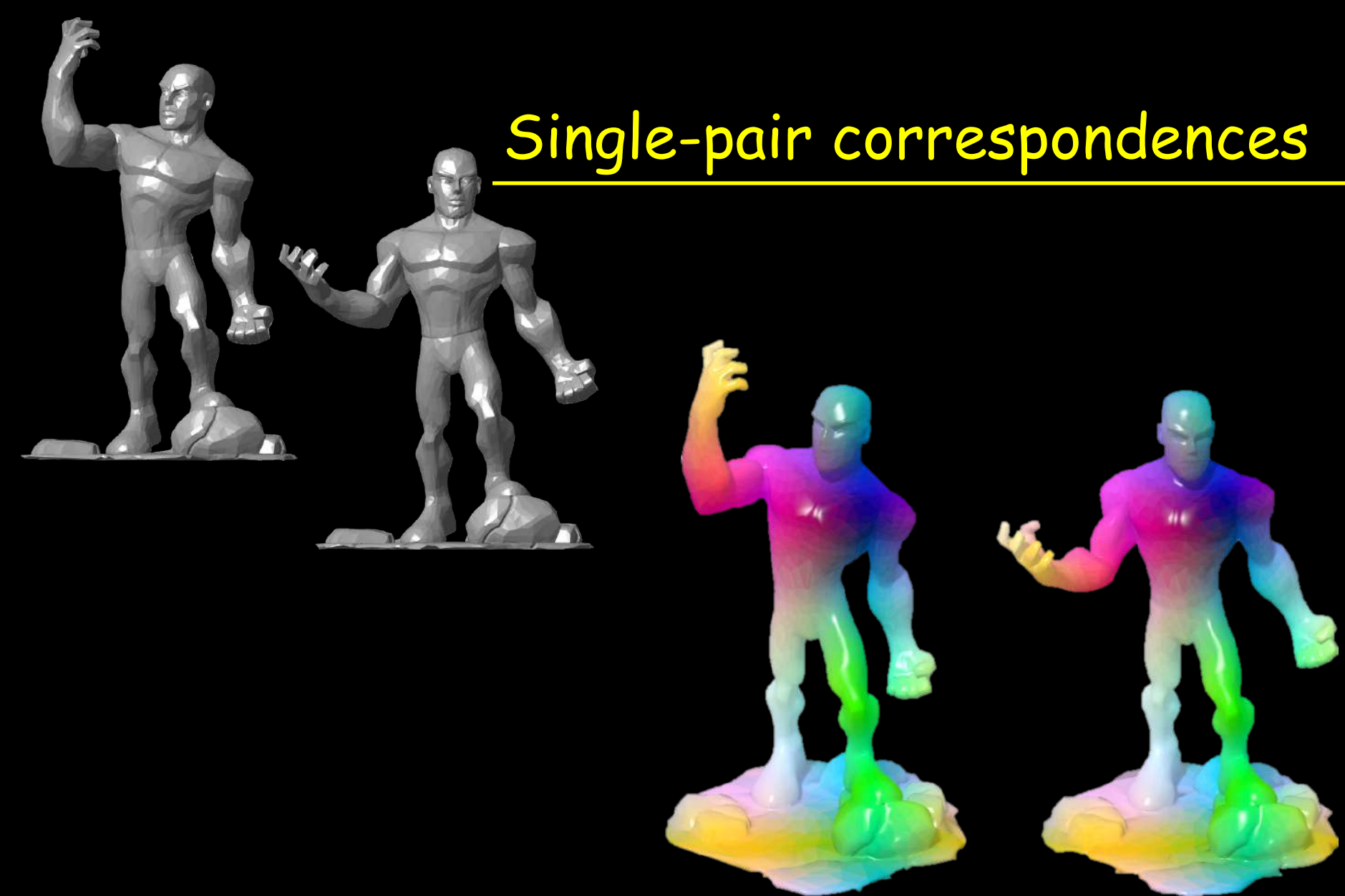


Partial Correspondence

Geodesic Error



Single-pair correspondences

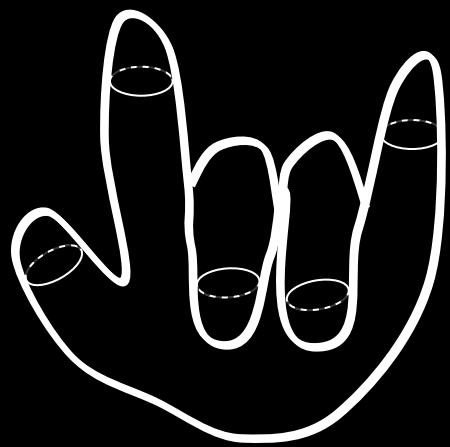
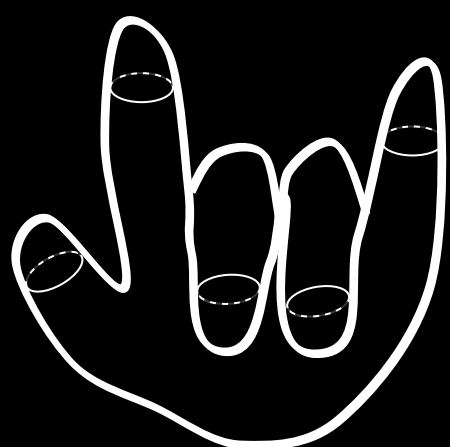
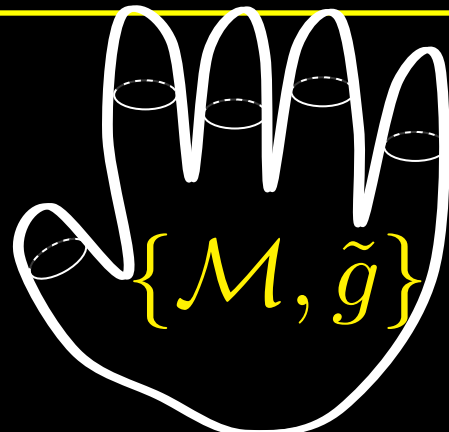


Manifold vs. Riemannian Manifolds

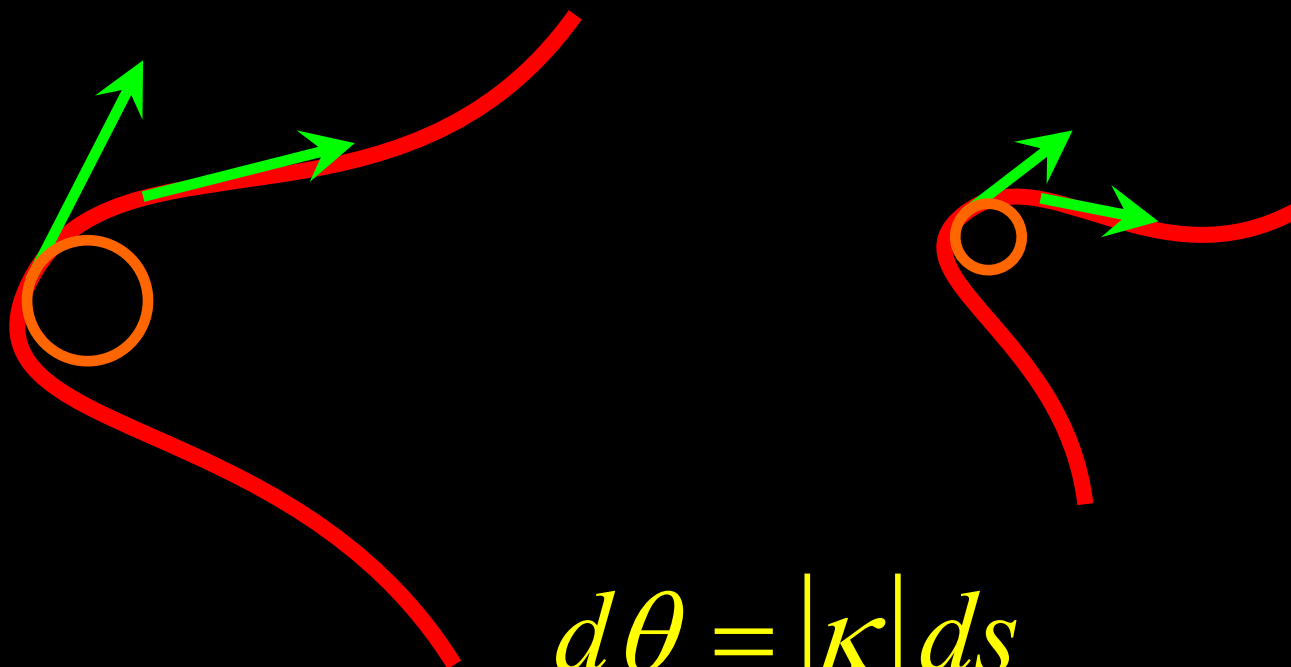
$$\Delta_g \psi_i = \lambda_i \psi_i$$

$$\Delta_{\tilde{g}} \tilde{\psi}_i = \tilde{\lambda}_i \tilde{\psi}_i$$

$$C_{ij} = \langle \psi_i, \tilde{\psi}_j \rangle_{\tilde{g}}$$



Scale invariance?



$$d\theta = |\kappa| ds$$

Surface Laplacian

$$\Delta_{\tilde{g}} \equiv -\frac{1}{\sqrt{\tilde{g}}} \partial_i \sqrt{\tilde{g}} \tilde{g}^{ij} \partial_j$$



$$\tilde{g}_{ij} = | \kappa_1 \kappa_2 | \langle S_i, S_j \rangle$$

Eigenfunctions

$$g_{ij} = \langle S_{\omega_i}, S_{\omega_j} \rangle$$

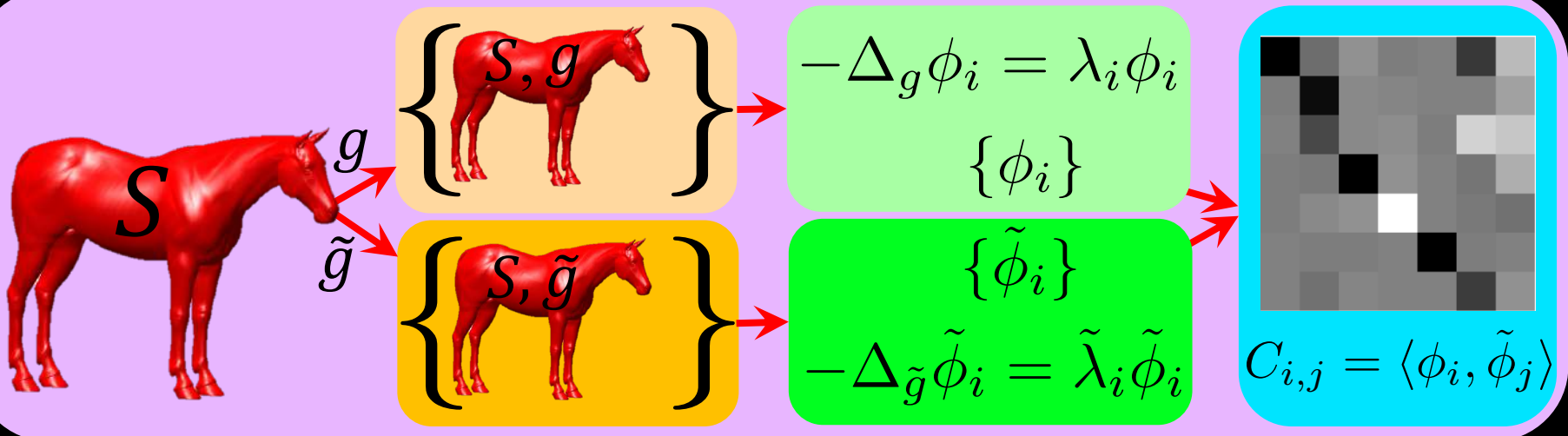
$$-\Delta_g \psi_i = \lambda_i \psi_i$$



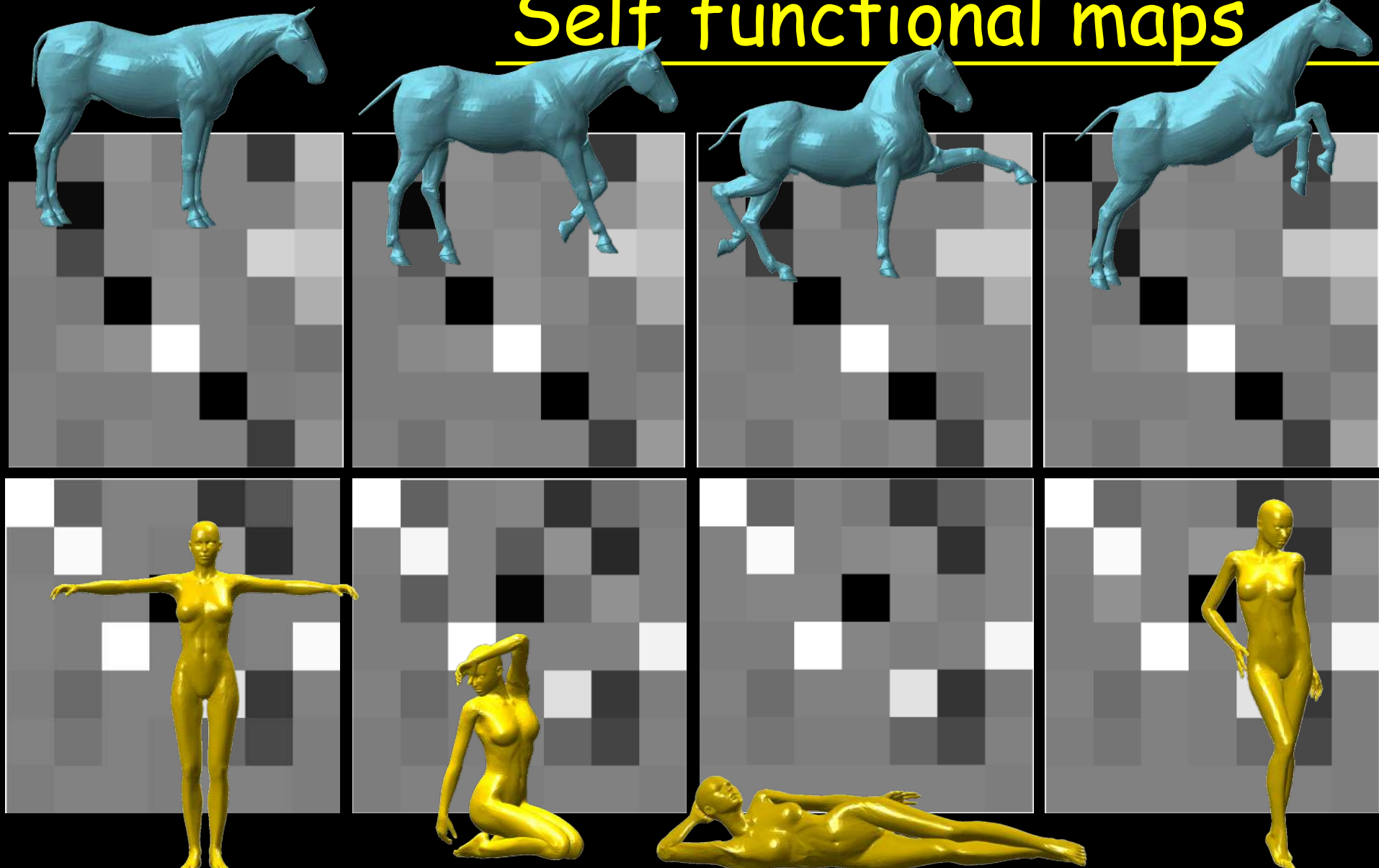
$$\tilde{g}_{ij} = |K| g_{ij}$$

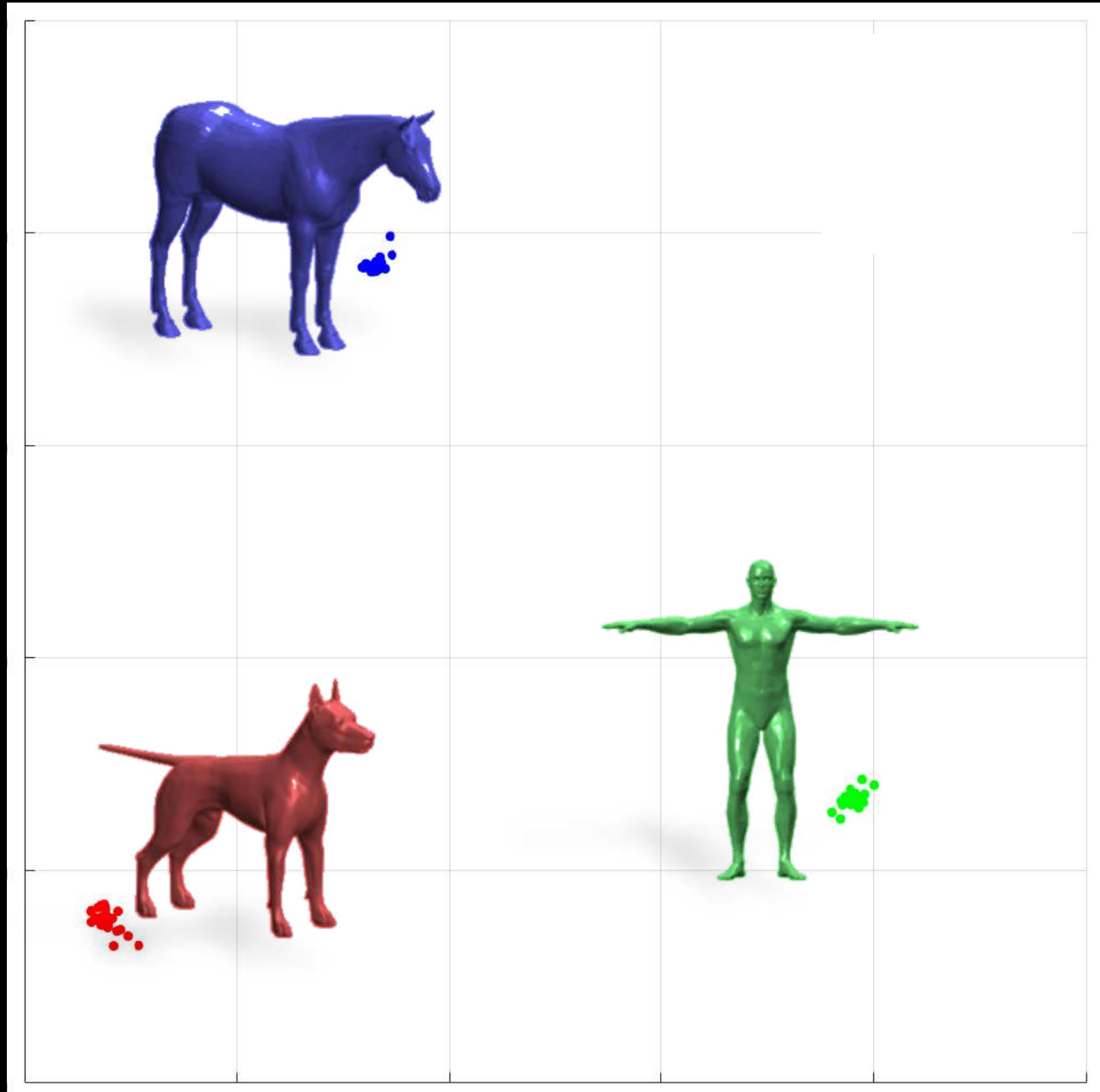
$$-\Delta_{\tilde{g}} \tilde{\psi}_i = \tilde{\lambda}_i \tilde{\psi}_i$$

Self functional maps



Self functional maps

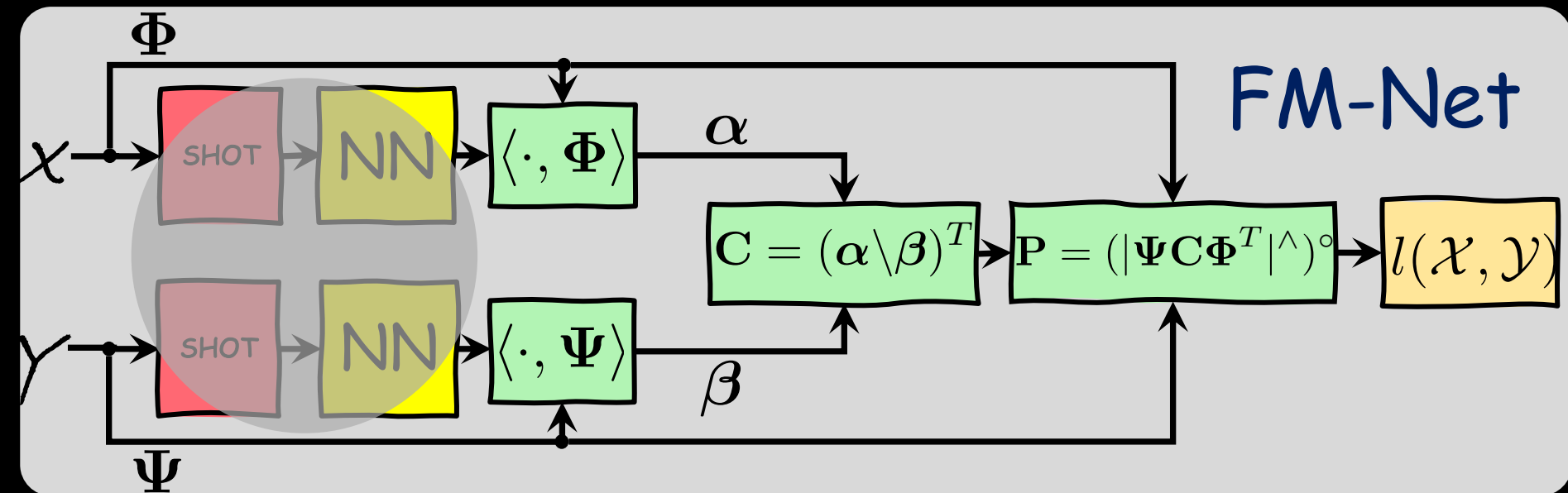






Unsupervised Functional Maps-Net

$$l_{uns}(\mathcal{X}, \mathcal{Y}) = \|D_{\mathcal{X}} - P D_{\mathcal{Y}} P^T\|$$



Ovsjanikov et al. 2012

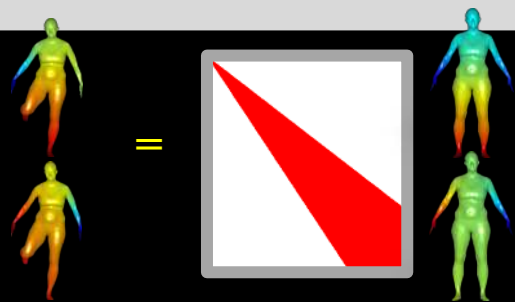
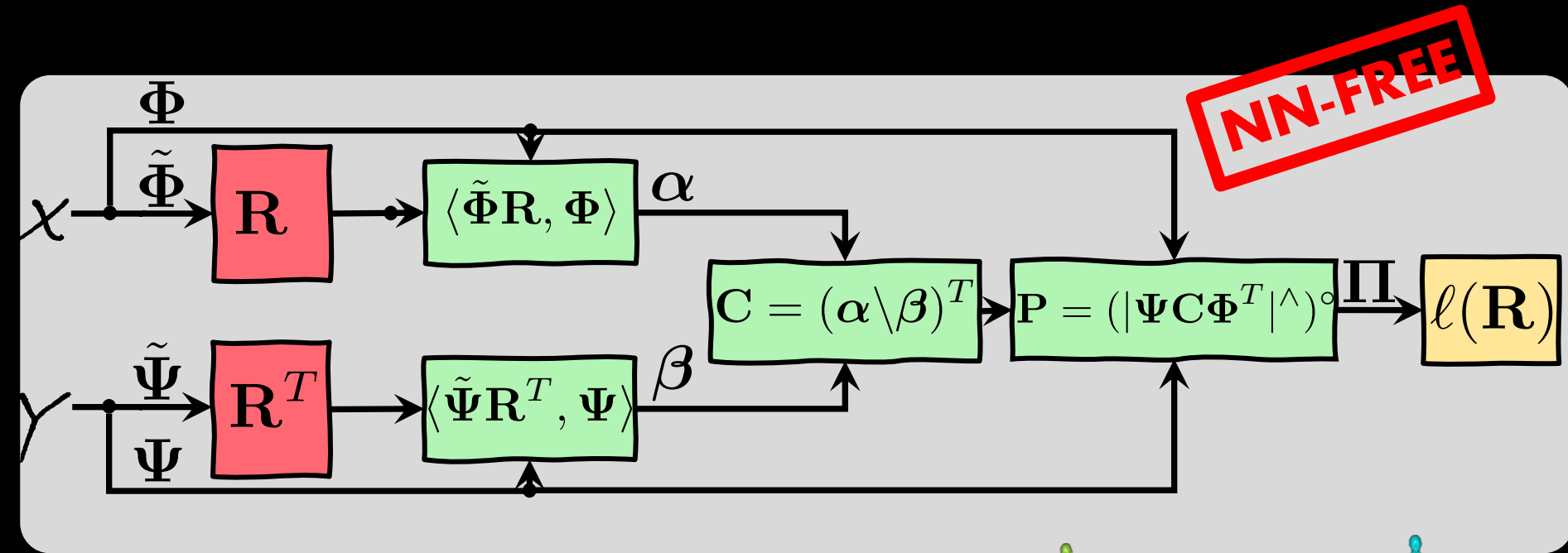
Litany, Remez, Rodola, A Bronstein, M Bronstein ICCV'17

Halimi, Litany, Rodola, A Bronstein, K. CVPR'19

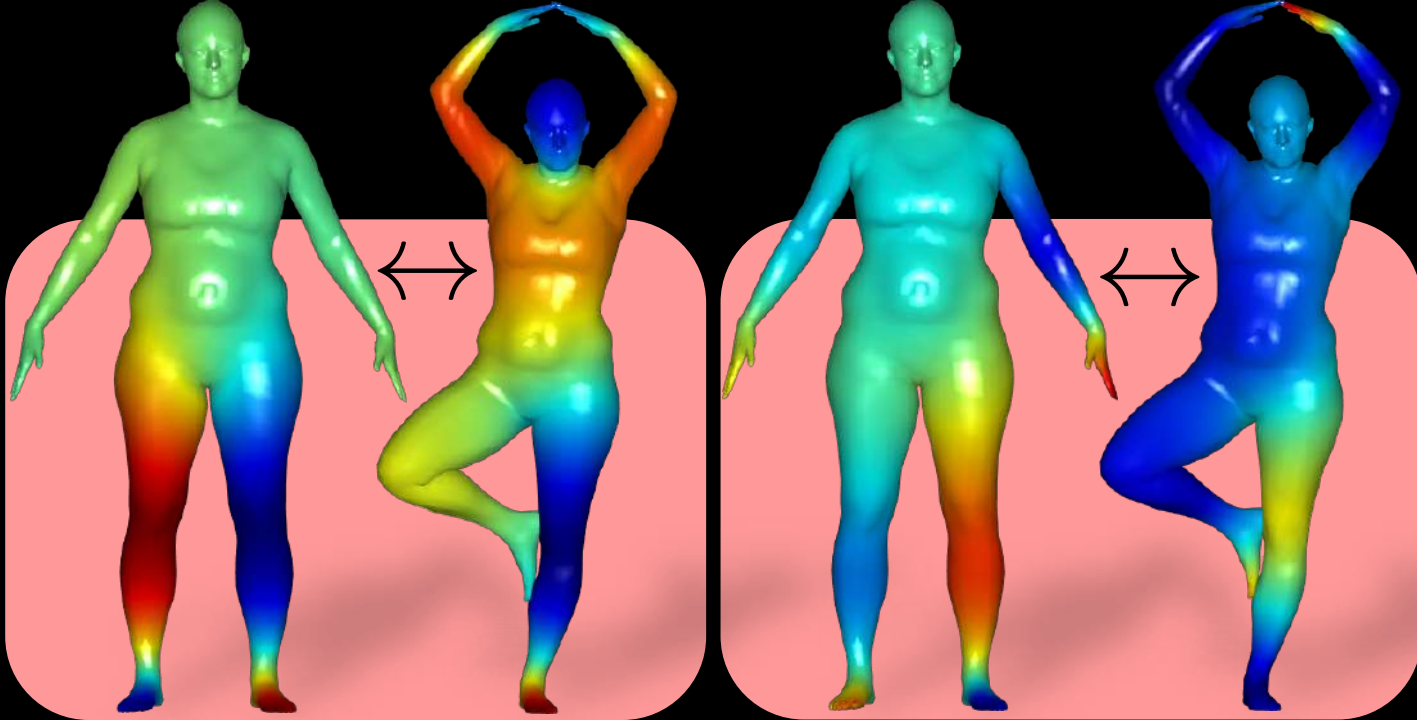
Roufosse, Sharma, Ovsjanikov, ICCV'19

Aligning scale-invariant LBO eigenfunctions

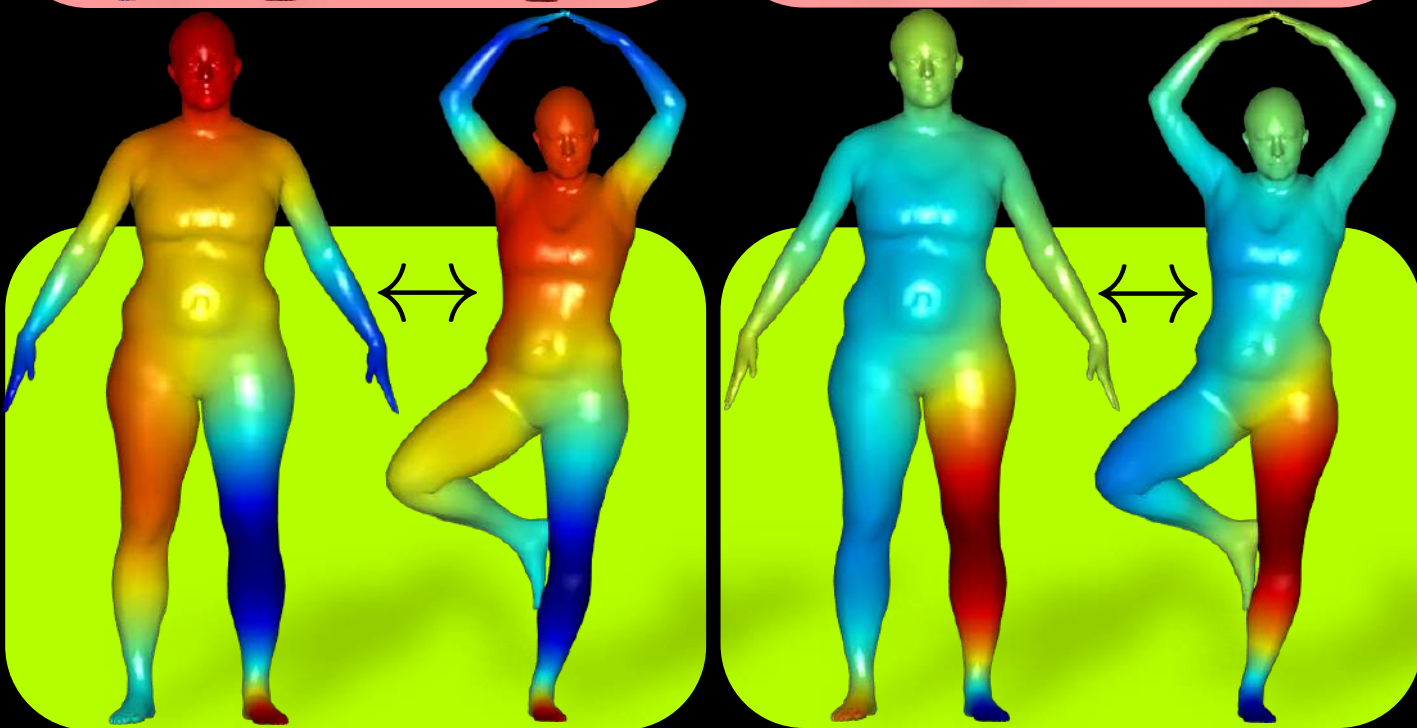
$$l_{uns}(\mathcal{X}, \mathcal{Y}) = \|D_{\mathcal{X}} - P D_{\mathcal{Y}} P^T\|$$



Before

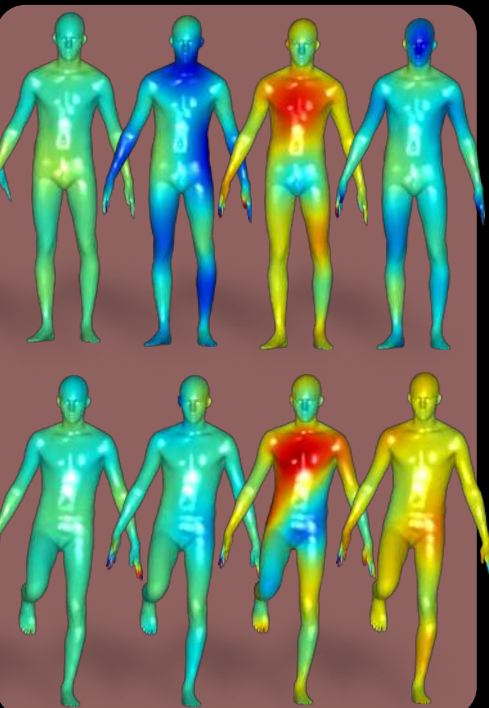
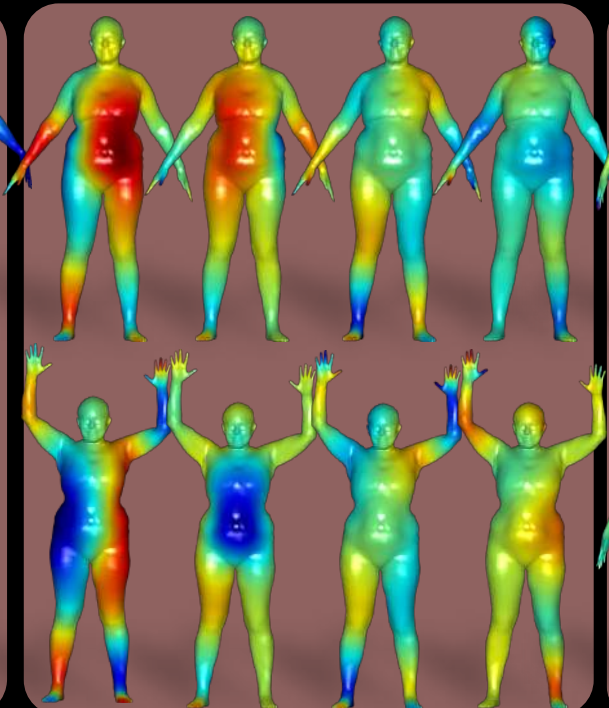


After

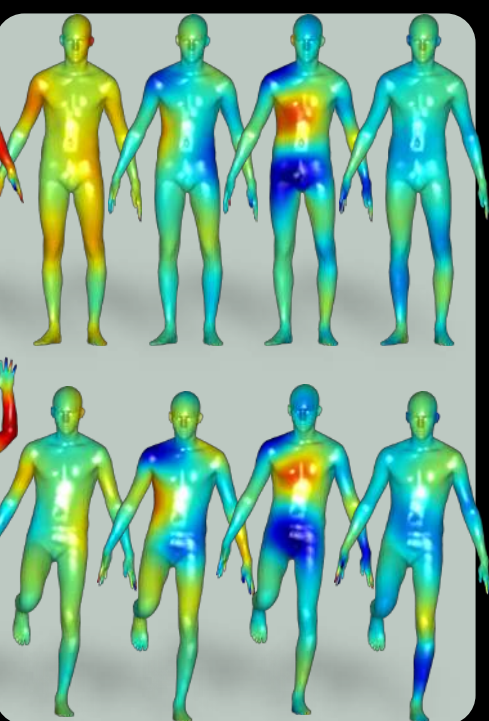
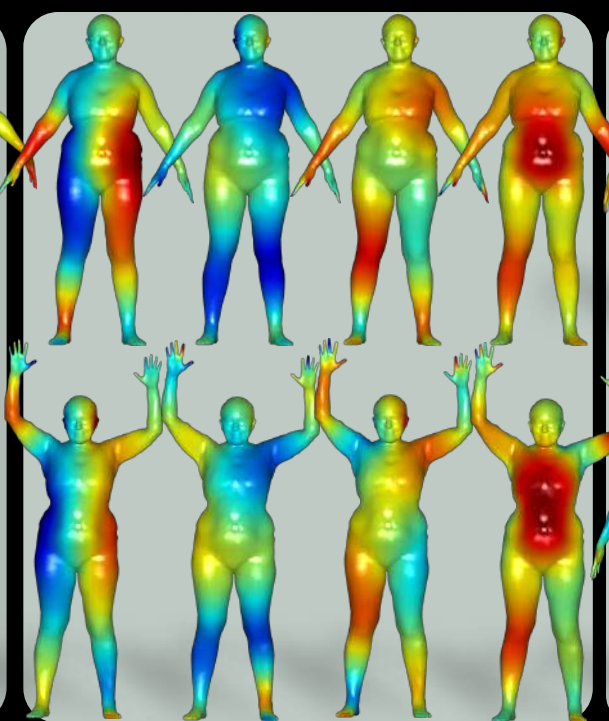
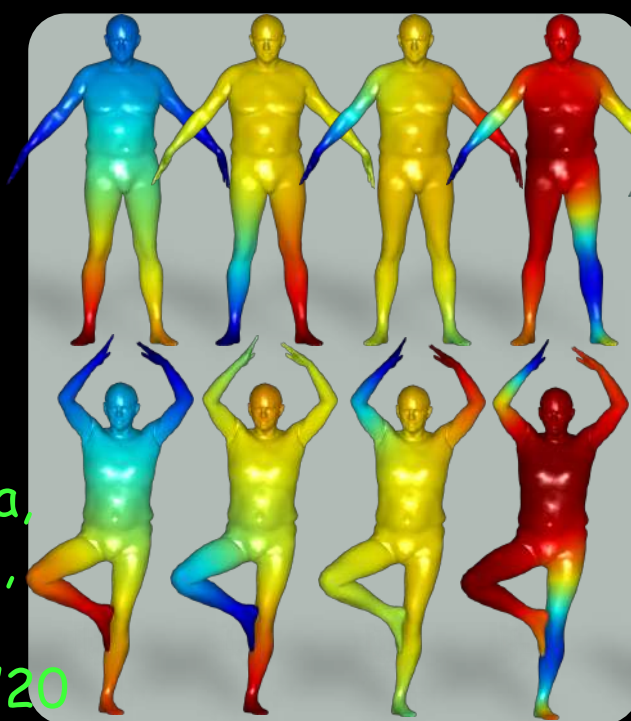


Bracha, Halimi,
K. 3DOR'20

Before



After



Bracha,
Halimi,
K.
3DOR'20



*Thank you for
your attention*

